

RD-A166 103

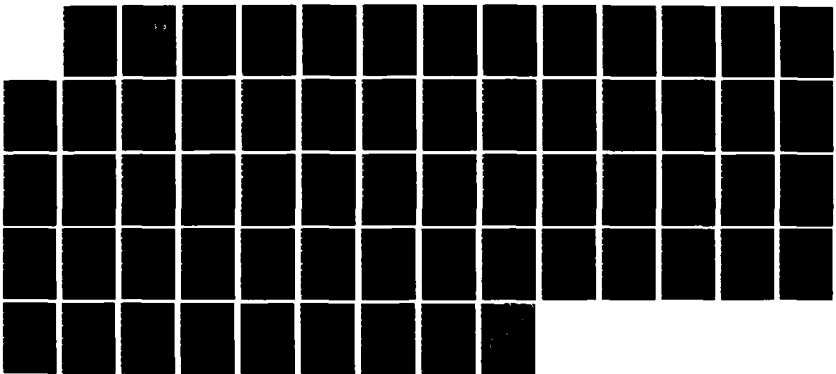
AN EVALUATION OF POTENTIAL MODIFICATIONS TO THE SEER  
(SIMPLIFIED ESTIMATI. (U) SCIENCE APPLICATIONS

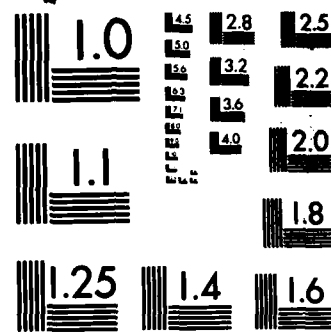
1/1

INTERNATIONAL CORP MCLEAN VA R C EDWARDS 01 SEP 83  
SAI-83/1176 DNA-RR-84-311 DNA001-88-C-0047 F/G 15/6

UNCLASSIFIED

NL





MICROCOPY RESOLUTION TEST CHART  
NATIONAL BUREAU OF STANDARDS-1963-A

AD-A166 103

DNA-TR-84-311

**AN EVALUATION OF POTENTIAL MODIFICATIONS TO  
THE SEER FALLOUT CODE**

R. C. Edwards  
Science Applications International Corporation  
P. O. Box 1303  
McLean, VA 22102-1303

1 September 1983

Technical Report

12  
DTIC  
SELECTED  
APR 10 1988  
S D

**CONTRACT No. DNA 001-80-C-0047**

Approved for public release;  
distribution is unlimited.

THIS WORK WAS SPONSORED BY THE DEFENSE NUCLEAR AGENCY  
UNDER RDT&E RMSS CODE B364080464 V99QAXNJ31203 H2590D.

Prepared for  
Director  
DEFENSE NUCLEAR AGENCY  
Washington, DC 20305-1000

DTIC FILE COPY

86 2 7 316

Destroy this report when it is no longer needed. Do not return to sender.

PLEASE NOTIFY THE DEFENSE NUCLEAR AGENCY,  
ATTN: STTI, WASHINGTON, DC 20305-1000, IF YOUR  
ADDRESS IS INCORRECT, IF YOU WISH IT DELETED  
FROM THE DISTRIBUTION LIST, OR IF THE ADDRESSEE  
IS NO LONGER EMPLOYED BY YOUR ORGANIZATION.



UNCLASSIFIED

SECURITY CLASSIFICATION OF THIS PAGE

AD-A166103

Form Approved  
OMB No. 0704-0188  
Exp. Date: Jun 30, 1986

REPORT DOCUMENTATION PAGE			
1a. REPORT SECURITY CLASSIFICATION <b>UNCLASSIFIED</b>		1b. RESTRICTIVE MARKINGS	
2a. SECURITY CLASSIFICATION AUTHORITY <b>N/A since Unclassified</b>		3. DISTRIBUTION/AVAILABILITY OF REPORT <b>Approved for public release; distribution is unlimited.</b>	
2b. DECLASSIFICATION/DOWNGRADING SCHEDULE <b>N/A since Unclassified</b>		4. PERFORMING ORGANIZATION REPORT NUMBER(S) <b>SAI-83/1176</b>	
6a. NAME OF PERFORMING ORGANIZATION <b>Science Applications International Corporation</b>	6b. OFFICE SYMBOL (If applicable)	5. MONITORING ORGANIZATION REPORT NUMBER(S) <b>DNA-TR-84-311</b>	
6c. ADDRESS (City, State, and ZIP Code) <b>P. O. Box 1303 McLean, VA 22102-1303</b>		7a. NAME OF MONITORING ORGANIZATION <b>Director Defense Nuclear Agency</b>	
8a. NAME OF FUNDING / SPONSORING ORGANIZATION		8b. OFFICE SYMBOL (If applicable)	
8c. ADDRESS (City, State, and ZIP Code)		9. PROCUREMENT INSTRUMENT IDENTIFICATION NUMBER <b>DNA 001-80-C-0047</b>	
		10. SOURCE OF FUNDING NUMBERS	
		PROGRAM ELEMENT NO <b>62715H</b>	PROJECT NO <b>V99QAXN</b>
		TASK NO <b>J</b>	WORK UNIT ACCESSION NO. <b>DH004601</b>
11. TITLE (Include Security Classification) <b>AN EVALUATION OF POTENTIAL MODIFICATIONS TO THE SEER FALLOUT CODE</b>			
12. PERSONAL AUTHOR(S) <b>Edwards, R. C.</b>			
13a. TYPE OF REPORT <b>Technical Report</b>	13b. TIME COVERED <b>FROM 820801 TO 830801</b>	14. DATE OF REPORT (Year, Month, Day) <b>830901</b>	15. PAGE COUNT <b>62</b>
16. SUPPLEMENTARY NOTATION <b>This work was sponsored by the Defense Nuclear Agency under RDT&amp;E RMSS Code B364080464 V99QAXNJ31203 H2590D.</b>			
17. LOSATI CODES		18. SUBJECT TERMS (Continue on reverse if necessary and identify by block number) <b>Radioactive Fallout DELFIC Fallout Computer Code CIVIC SEER</b>	
FIELD <b>9</b>	GROUP <b>2</b>		
18	8		
19. ABSTRACT (Continue on reverse if necessary and identify by block number)  <p>This effort concludes that the current CIVIC version of SEER with adjusted K-factor is the best available fast-running approximation to DELFIC. This conclusion was reached after investigating a trial methodology which was developed for the SEER fallout code in order to conserve total fallout activity and improve the approximation to DELFIC results. The trial methodology was compared with DELFIC and also with the CIVIC version of SEER, which utilizes an adjusted K-factor to improve the approximation to DELFIC. Also, the particle size group activity distribution currently used in SEER was replaced by one approximately the same as that used in DELFIC. Combinations of trial and old methodology with trial and old activity distributions were all run for comparison with DELFIC. The results of the comparison show that:</p> <ul style="list-style-type: none"><li>• The trial methodology conserves activity while utilizing the original K-factor.</li></ul>			
20. DISTRIBUTION/AVAILABILITY OF ABSTRACT <input type="checkbox"/> UNCLASSIFIED/UNLIMITED <input checked="" type="checkbox"/> SAME AS RPT <input type="checkbox"/> DTIC USERS		21. ABSTRACT SECURITY CLASSIFICATION <b>UNCLASSIFIED</b>	
22a. NAME OF RESPONSIBLE INDIVIDUAL <b>Betty L. Fox</b>		22b. TELEPHONE (Include Area Code) <b>(202) 325-7042</b>	22c. OFFICE SYMBOL <b>DNA/STTI</b>

UNCLASSIFIED

SECURITY CLASSIFICATION OF THIS PAGE

- The trial methodology produces fallout contours which are a better approximation to DELFIC than are those produced by the old SEER with the original K-factor.
- The current CIVIC version of SEER with the adjusted K-factor is a slightly better approximation to DELFIC than the new methodology.
- The trial methodology requires on the average, about 20% additional computer run time.
- The trial particle size group activity distribution reduces the size of the close-in contours and allows a slight improvement to the SEER/CIVIC approximation to DELFIC at the 3000 r/hr contour, and a slightly less accurate approximation at the 100 and 300 r/hr contours.

It is possible that further work on the trial methodology could improve the approximation to DELFIC.

## SUMMARY

A trial methodology was developed for the SEER fallout code in order to conserve total fallout activity and improve the approximation to DELFIC results. The trial methodology was compared with DELFIC and also with the CIVIC version of SEER, which utilizes an adjusted K-factor to improve the approximation to DELFIC. Also, the particle size group activity distribution currently used in SEER was replaced by one approximately the same as that used in DELFIC. Combinations of trial and old methodology with trial and old activity distributions were all run for comparison with DELFIC. The results of the comparison show that:

- The trial methodology conserves activity while utilizing the original K-factor.
- The trial methodology produces fallout contours which are a better approximation to DELFIC than are those produced by the old SEER with the original K-factor.
- The current CIVIC version of SEER with the adjusted K-factor is a slightly better approximation to DELFIC than the trial methodology.
- The trial methodology requires on the average, about 20% additional computer run time.
- The new particle size group activity distribution reduces the size of the close-in contours and allows a slight improvement to the SEER/CIVIC approximation to DELFIC at the 3000 r/hr contour, and a slightly less accurate approximation at the 100 and 300 r/hr contours.

It is possible that further work on the trial methodology could improve the approximation to DELFIC. Pending this, however, it is concluded from this effort and the results of Reference 1 that the current CIVIC version of SEER with adjusted K-factor is the best available fast-running approximation to DELFIC.

Accession For	
NTIS	CRA&I <input checked="" type="checkbox"/>
DTIC	TAB <input type="checkbox"/>
Unannounced <input type="checkbox"/>	
Justification .....	
By .....	
Distribution /	
Availability Codes	
Dist	Avail and/or Special
A-1	



## TABLE OF CONTENTS

<u>SECTION</u>		<u>PAGE</u>
	<b>SUMMARY .....</b>	1
	<b>LIST OF ILLUSTRATIONS.....</b>	3
	<b>LIST OF TABLES .....</b>	5
1	<b>INTRODUCTION .....</b>	7
2	<b>CURRENT SEER APPROACH .....</b>	8
3	<b>MODIFIED APPROACH .....</b>	13
	3-1 <b>Spread of Fallout Activity from One Disc (Subroutine SMEAR) .....</b>	13
	3-2 <b>Setting up the Fallout Map (Sub routine GRID) .....</b>	25
	3-3 <b>Calculating the Fallout Activity Density at Each Map Point (Subroutine MAPDEN) ....</b>	27
	3-4 <b>Plotting the Map (Subroutine PLTMAP).....</b>	29
	3-5 <b>Summary of Subroutines Added and Replaced .....</b>	30
	3-6 <b>New Particle Size Group Activity Distribution .....</b>	30
4	<b>COMPARISON RESULTS .....</b>	31
	4-1 <b>Phase One Results - Comparison with Pre-CIVIC SEER .....</b>	31
	4-2 <b>Phase Two Results - Comparisons with CIVIC Version of SEER .....</b>	48
5	<b>CONCLUSIONS.....</b>	55
6	<b>REFERENCES .....</b>	56

## LIST OF ILLUSTRATIONS

<u>FIGURE</u>		<u>PAGE</u>
2-1	Cylindrical stabilized debris cloud used by SEER .....	9
2-2	Example of landing pattern for the SEER particle classes .....	10
2-3	Location of key points in the SEER fallout pattern .....	11
3-1	Representative SEER results following subroutine SEER 2.....	14
3-2	Spread of activity from disc (IB, IA) .....	15
3-3	Detail for finding the tangent points P11, P12, P21, P22, P31, P32, P41, P42.....	19
3-4	Possible orientations of quadrangle sides S1', S2', S3', S4' .....	20
3-5	Illustration of corner areas excluded in activity spread .....	24
3-6	Illustration of cross-product method of determining if a map point is within quadrangle area .....	28
4-1	10 r/hr contour, DELFIC vs. old SEER .....	34
4-2	10 r/hr contour, DELFIC vs. modified SEER .....	35
4-3	10 r/hr contour, DELFIC vs. modified SEER, new activity distribution .....	36
4-4	100 r/hr contour, DELFIC vs. old SEER.....	37
4-5	100 r/hr contour, DELFIC vs. old SEER, new activity distribution..	38
4-6	100 r/hr contour, DELFIC vs. modified SEER .....	39
4-7	100 r/hr contour, DELFIC vs. modified SEER, new activity distribution .....	40
4-8	1000 and 3000 r/hr contours, DELFIC vs. old SEER .....	41
4-9	1000 and 3000 r hr contours, DELFIC vs. old SEER, new activity distribution .....	42
4-10	1000 and 3000 r hr contours, DELFIC vs. modified SEER .....	43
4-11	1000 and 3000 r hr contours, DELFIC vs. modified SEER, new activity distribution .....	44

## LIST OF ILLUSTRATIONS (cont'd)

<u>FIGURE</u>		<u>PAGE</u>
4-12	Contour areas, DELFIC vs. old SEER .....	49
4-13	Contour areas, DELFIC vs. CIVIC SEER .....	50
4-14	Contour areas, DELFIC vs. CIVIC SEER, new activity distribution .....	51
4-15	Contour areas, DELFIC vs modified SEER .....	52
4-16	Contour areas, DELFIC vs. modified SEER, new activity distribution .....	54

## LIST OF TABLES

<u>TABLE</u>		<u>PAGE</u>
3-1	Equations for the tangent points P12, P21 for all orientations of S1.....	22
4-1	Summary of results from DELFIC and SEER .....	32
4-2	Initial activity values from the literature .....	45



## SECTION I

### INTRODUCTION

This report presents the methodology and results of an attempt to modify and improve the computer code SEER (Simplified Estimation of Exposure to Radiation). SEER is part of the large nuclear weapon damage assessment code CIVIC. SEER (References 2, 3) was developed in the early 1970s with the intent that it simulate the fallout exposure rate contours of DELFIC (Defense Land Fallout Interpretive code) while using a minimal amount of computer time.

A problem that surfaced with the development of SEER was the fact that the SEER methodology (see Section 2) leads to an overprediction of the total activity deposited on the ground (see References 4, 5). In order to compensate for this characteristic, SAI has lowered the value of the K-factor in the SEER portion of CIVIC to approximately half of the original value. The K-factor is the amount of weapon fallout activity per unit yield, distributed over unit area (see Section 4-1.3). Its value is not precisely known, in part because the percentage of total radioactive debris that constitutes early fallout (as opposed to that which is lofted to high altitudes and carried off beyond local fallout distances) is not well known and varies with height of burst and other conditions. The original K-factor used in SEER (Reference 3, p. 15) is taken from Reference 6. The value indicated by Reference 7 is about 25% lower than this.

This work effort investigated the possibility of modifying the SEER methodology so that activity is conserved and a good approximation to DELFIC results could be obtained without resort to the adjustment of the K-factor. The following sections describe the current SEER methodology, the trial methodology, and the results of the comparison.

## SECTION 2

### CURRENT SEER APPROACH

As shown in Figure 2-1, SEER considers a cylindrical stabilized cloud and divides it into (NLVL-1) slabs, the number depending on the weapon yield. The cloud is further discretized by dividing the activity among 25 particle groups (subscript IB), each of which is assigned a fraction of the total activity as well as characteristic fall times from various altitudes. The assumption is made that each altitude slab has an equal share of the total activity, and that the particle distribution is the same in each altitude slab. SEER calculates the ground locations and radii of 25 x NLVL discs, each disc originating at one of the discreet slab boundary altitudes corresponding to IA= 1,2, ...NLVL. The situation is shown in Figure 2-2, where the A,B,C,... "hot lines" correspond to altitude levels IA = 1,2,3..., and the disc landing points 1,2,3,4...correspond to the various particle size groups IB = 1,2,3,...25. SEER computes the landing points of the centers of each disc. The activity densities of the discs are calculated using an area spread which is a multiple of the disc diameter and a fraction of the distance from the GZ or from the previous disc (SEER 3.51-SEER 3.92). Subsequent activity densities are calculated using a log smoothing procedure. Following these calculations is an entire set of calculations which compute the fallout densities at a set of "key points", as illustrated in Figure 2-3. The rationale stated for this additional step is... "so that an appropriate network of exposure-rate values will be available for the mapping routines." Consideration of contributions from more than one disc to each key point is limited solely to discs from adjacent altitude-level "hot lines" that lie within a disc radius of the key point. Moreover, this is done only for discs of the same particle class. As might be suggested by Figure 2-2, this whole procedure can lead to "gaps" of no activity density between discs. Overestimation of total fallout activity occurs when the activity of map points that fall in these gaps is "filled in" through the SEER process of interpolating between key points to arrive at map point activity densities. In summary, the possible causes of inaccuracies in SEER are as follows:

- Initial use of an incorrect area (SEER 3.79) spread (or "smear") of activity from one disc, based only on the diameter of the disc itself and its distance from the GZ or the previous disc (SEER 3.51-SEER 3.92).

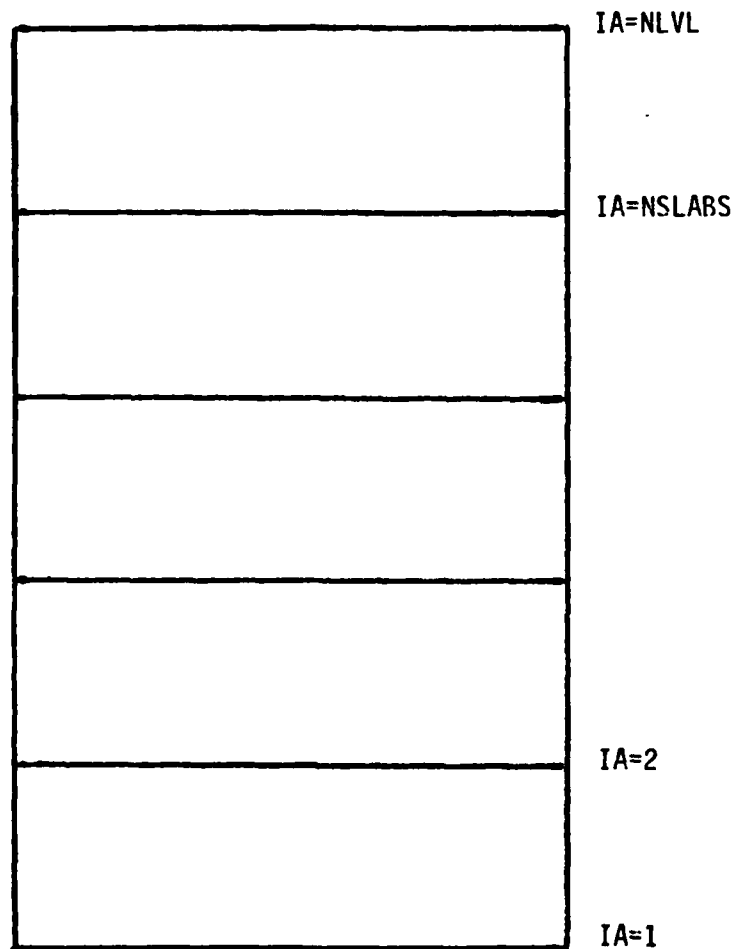
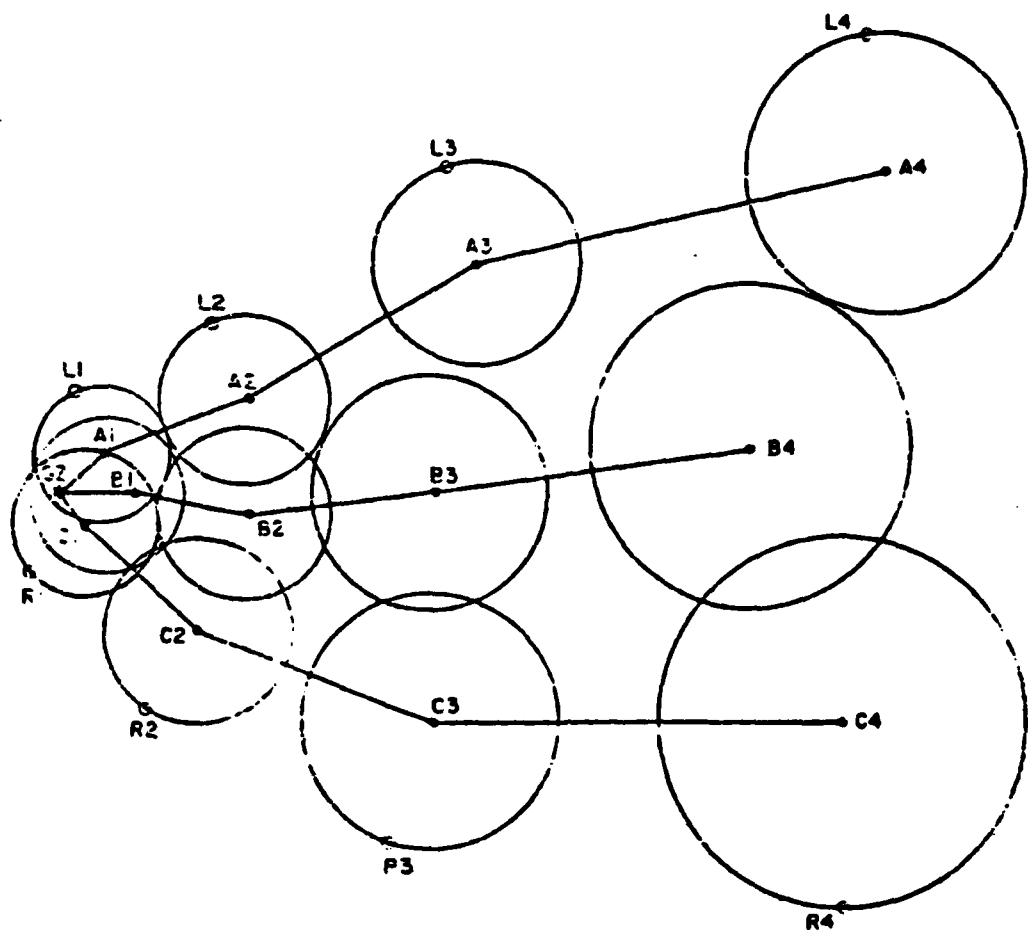


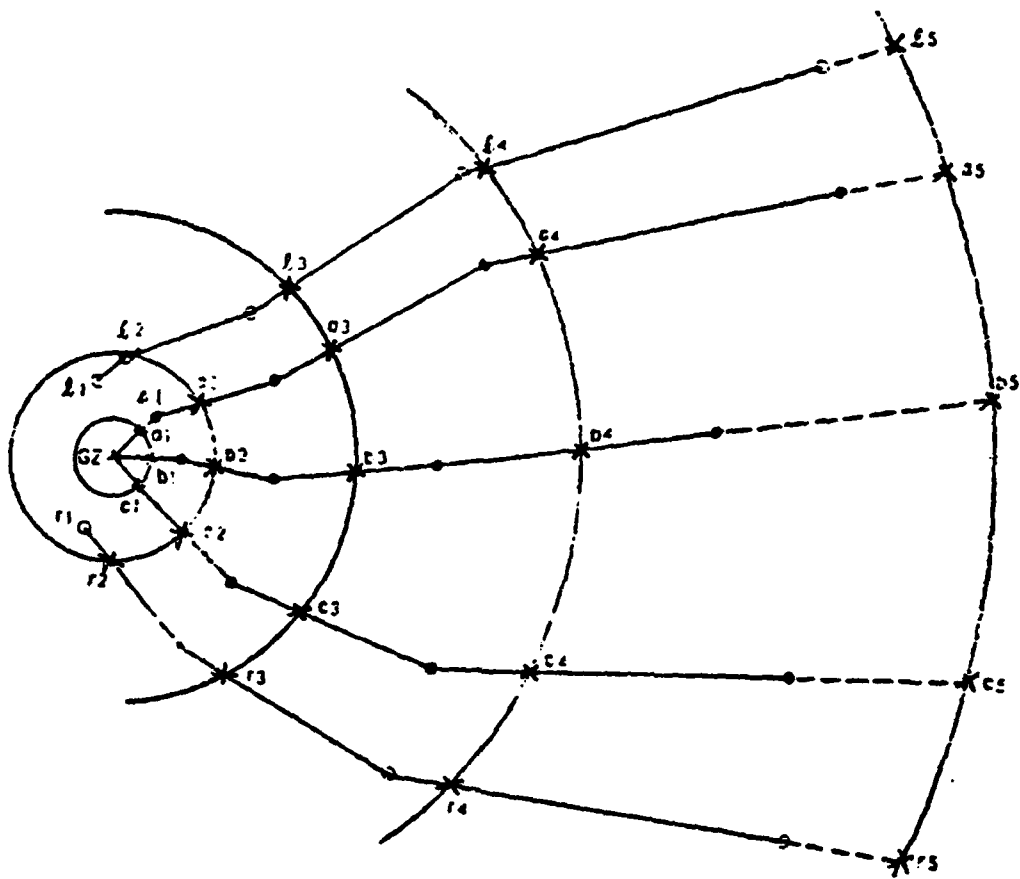
Figure 2-1. Cylindrical stabilized debris cloud used by SEER.



- PARTICLE CLASS LANDING POINTS
- PATTERN EDGE POINTS

Note: Paths A, B, and C are the particle class paths for 3 cloud levels. The example shows only 4 particle classes but the SEER model uses 25 particle classes. The L and R points are along the left and right edges of the fallout pattern.

Figure 2-2. Example of landing pattern for the SEER particle classes.



- PARTICLE CLASS LANDING POINTS
- PATTERN EDGE POINTS
- ✗ FALLOUT PATTERN KEY POINTS

Figure 2-3. Location of key points in the SEER fallout pattern.

- Failure to consider contributions of discs from other particle size groups to the activity at the given point (either disc impact point or "key point") (SEER 3).
- Failure to consider contributions of discs from other altitude levels beyond disc radius distance (SEER 3).
- "Filling in" of activity by interpolation at locations where the activity may not exist (or be less than the interpolated value).

It is also true that SEER does not include a model for the cloud stem. This would tend to lower the amount of close-in fallout, but SEER compensates (to a certain degree) for this by utilizing a particle size group activity distribution which places more activity in the largest particle size groups than does DELFIC.

## SECTION 3

### MODIFIED APPROACH

In view of the considerations discussed in the previous section, an alternative approach is offered which will eliminate the entire SEER procedure following SEER 2, which calculates the positions and radii of the  $25 \times NLVL$  discs. The procedure which is substituted is discussed in the following sections. In brief, rather than establish intensities at arbitrary "key points" and determine map point intensities by interpolation, the substitute approach "smears" the activity from each disc over an area corresponding to altitude levels  $IA$  to  $IA+1$  and particle size groups  $IB-\frac{1}{2}$  to  $IB+\frac{1}{2}$ . Each quadrangular area (actually a "rounded off" quadrangle) is then investigated to determine which map grid points fall within it, and the intensity of the map grid point is augmented accordingly.

#### 3-1 SPREAD OF FALLOUT ACTIVITY FROM ONE DISC (SUBROUTINE SMEAR)

Consideration of the area over which the activity from one disc (say  $IB, IA$ ) should be spread can be facilitated by referring to Figure 3-1. SEER 2 calculates the positions  $XTAY (IB, IA)$ ,  $YTAY (IB, IA)$  for  $1 \leq IB \leq 25$  and  $1 \leq IA \leq NLVL$ . The disc radius  $RDTAY (IB, IA)$  is also calculated. The disc initial altitude is at the bottom of the finite altitude slab that it represents (see Figure 2-1). Thus, the activity from that slab is not confined to the  $IB, IA$  disc, but rather is distributed between that disc and the disc,  $IB, IA + 1$ , representing the next higher altitude slab. Moreover, the particle size group represented by the subscript  $IB$  is actually a range of particle sizes (e.g.,  $IB=1$  represents particles diameters in the range 2241-8768 microns). The fall times (read in as data statements in subroutine BLKONE) represent an average value over the size group. Therefore the  $IB, IA$  disc activity should also be spread over an area between the adjacent particle size groups  $IB-1$  and  $IB + 1$ . We thus arrive at an effective area "smear" of activity represented in Figure 3-2. The proper spread is enclosed in quadrangle  $P13, P23, P33, P43$ , with the hatched corner areas excluded. It might appear from Figure 3-2 that the use of this "outer quadrangle" would create an overlap strip with artificially high activity density. In reality, however, Figure 3-2

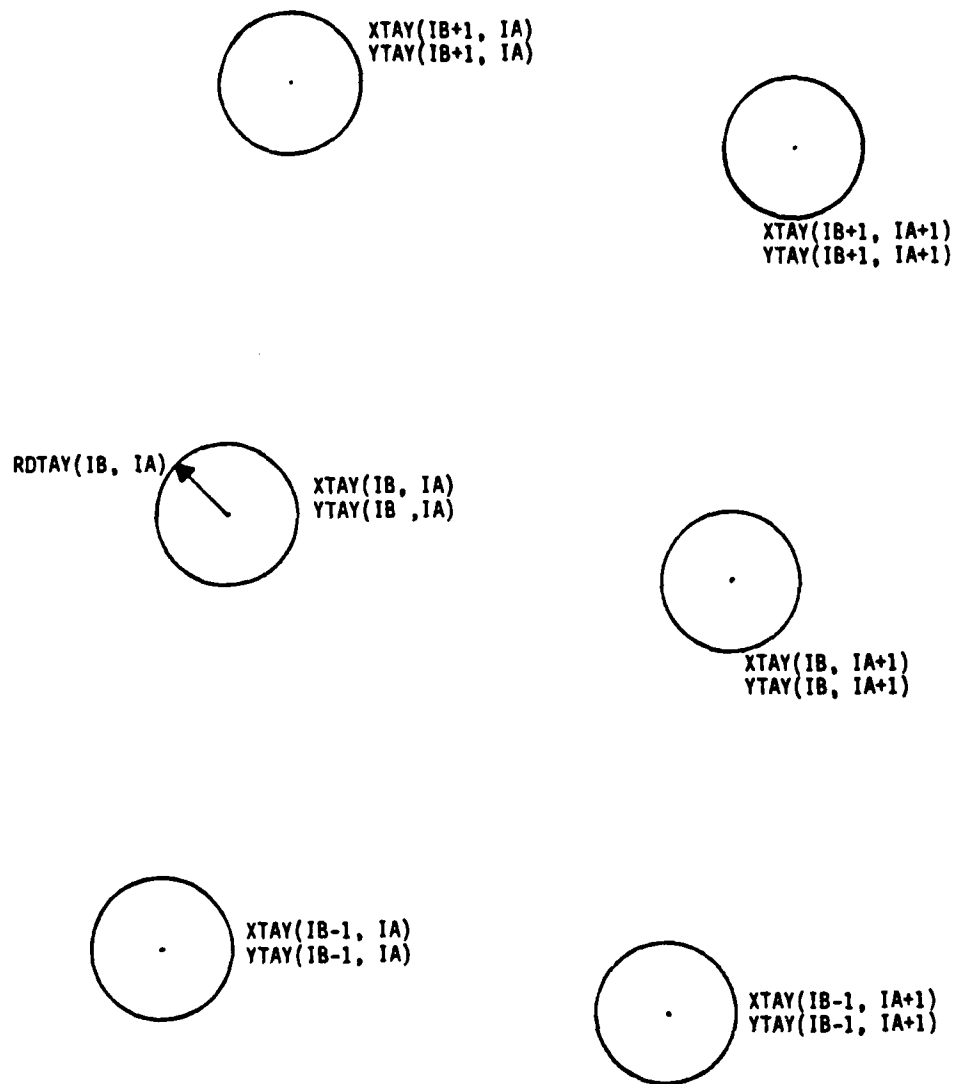


Figure 3-1. Representative SEER results following subroutine SEER 2.

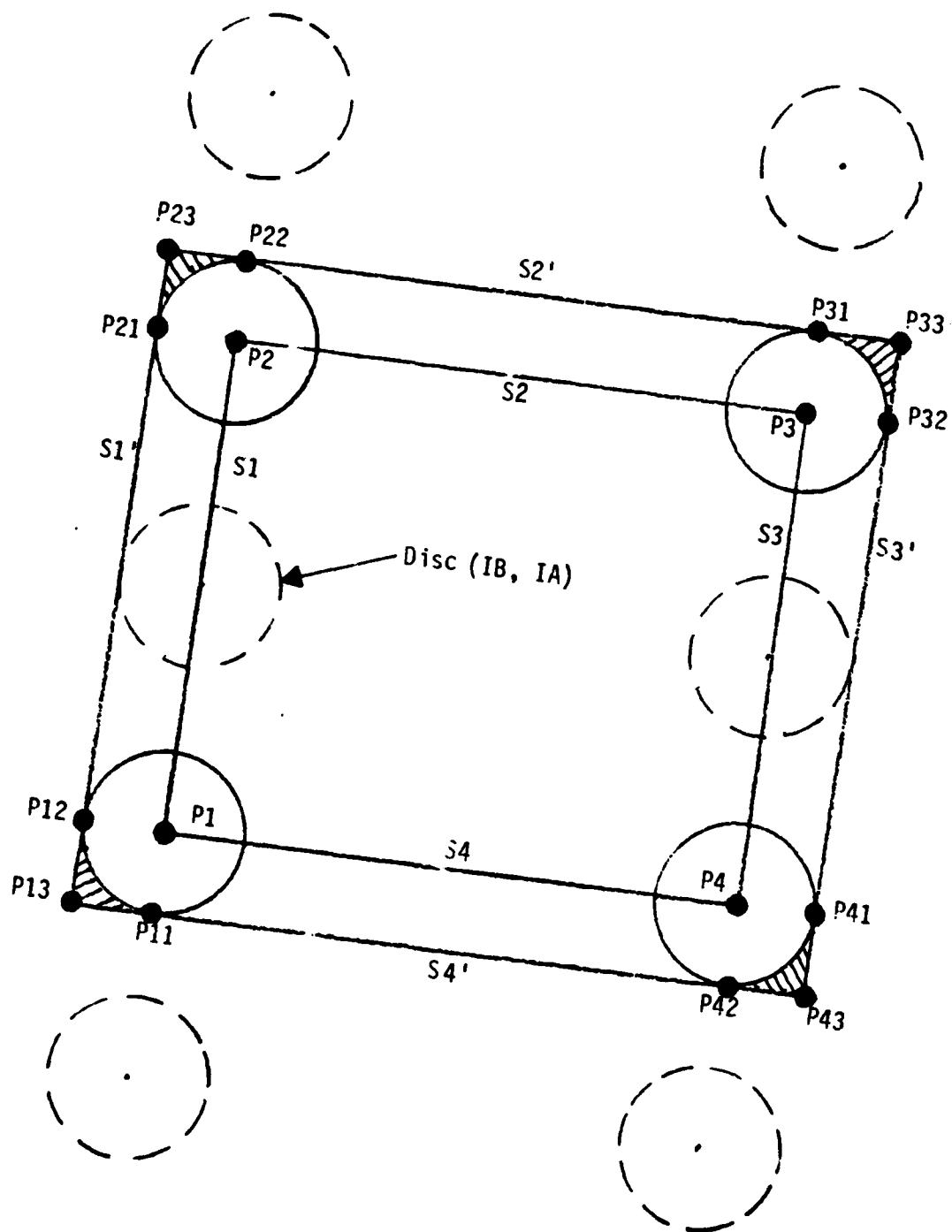


Figure 3-2. Spread of activity from disc (IB, IA).

represents only the situation for the very lightest of the particle groups. For most of the groups, there is considerable overlap of these "quadrangles" because the distances  $S_1, S_2, S_3, S_4$  are less (in some cases, much less) than the disc diameters. Even at the outer regions, where the lightest particles play a part, the overlap does not appear to present a problem. Indeed, the modified SEER provides a pattern which correlates well with that of DELFIC.

### 3-1.1 Finding the Points $P_1(X_1, Y_1)$ , $P_2(X_2, Y_2)$ , $P_3(X_3, Y_3)$ , and $P_4(X_4, Y_4)$

These points are approximated as midpoints between adjacent particle group wafer locations. Thus:

$$X_1 = (XTAY(IB-1, IA) + XTAY(IB, IA))/2.$$

$$X_2 = (XTAY(IB, IA) + XTAY(IB+1, IA))/2.$$

... etc.

However, if  $IB=1$ , we approximate as follows:

$$X_1 = XTAY(IB, IA) - DELTX$$

Where  $DELTX = X_2 - XTAY(IB, IA)$

...  $X_2$  having been calculated first.

If  $IB=25$ , we approximate as follows:

$$X_2 = XTAY(IB, IA) + DELTX$$

where  $DELTX = (XTAY(IB, IA) - XTAY(IB-1, IA))/2$

Analogous approximations are done for points  $P_3$  and  $P_4$ . Note that we do not have to make interpolation approximations for altitude increments. SEER has already calculated the location of the discs for  $IA=NLVL$ , which represents the upper limit for the top slab  $NSLABS=NLVL-1$ .

### 3-1.2 Calculating the Average Wafer Radius, R

Inspection of SEER output shows that over most of the particle size groups, the value of RDTAY (IB,IA) does not change drastically from one disc to the next. Thus, in the interest of conserving computer time, it is deemed sufficiently accurate to represent the disc radii corresponding to each of the points  $P_1, P_2, P_3, P_4$ , by a single disc size with a radius which is the average over the six discs shown in Figure 4-1, with discs IB,IA and IB, IA+1 each weighted twice.

### 3-1.3 Calculate the Cross-Products of Quadrangle $P_1P_2P_3P_4$

In order to locate map points in or out of the "rounded-off" quadrangle, it will be necessary to compare cross-product signs (see Section 3-3.2 below). It is therefore necessary to obtain the cross products of each side and its adjacent side. Since it is only the signs of the cross-products, not their value, that are important, it is sufficient to obtain the cross-products of the "inner" quadrangle ( $P_1, P_2, P_3, P_4$ ). As an example to illustrate the method for obtaining the cross-products, we will consider  $\underline{S_1} \times \underline{S_2}$ . For a two-dimensional cross-product (or vector-product) in the x-y plane, the cross product is obtained from:

$$\underline{S_1} \times \underline{S_2} = (a_1 b_2 - a_2 b_1) \underline{k}$$

where  $\underline{k}$  is the unit vector in the Z-direction (into or out-of the page), and the vectors are represented by:

$$\underline{S_1} = a_1 \underline{i} + b_1 \underline{j}$$

$$\underline{S_2} = a_2 \underline{i} + b_2 \underline{j}$$

where  $\underline{i}$  and  $\underline{j}$  are the unit vectors in the X and Y directions, respectively.

Now,

$$a_1 = X_2 - X_1 = DX_1 \text{ (in subroutine SMEAR)}$$

$$b_1 = Y_2 - Y_1 = DY_1$$

$$a_2 = X_3 - X_2 = DX_2$$

$$b_2 = Y_3 - Y_2 = DY_2$$

so  $\underline{S1} \times \underline{S2} = DX1 * DY2 - DX2 * DY1 = CPIX2$  (in subroutine SMEAR)

likewise  $CP2X3 = DX2 * DY3 - DX3 * DY2$   
 $CP3X4 = DX3 * DY4 - DX4 * DY3$   
 $CP4X1 = DX4 * DY1 - DX1 * DY4$

The cross-products are checked to see if they are .GT.0 or .LT.0 and if they all agree in sign. If they do not all agree in sign, then an error message is printed.

### 3-1.4 Locating the Tangent Points P11, P12, etc.

In order to construct the "outer" quadrangle of sides  $S_1' S_2' S_3' S_4'$ , the tangent points P11, P12, P21, P22, P31, P32, P41, P42 are first located (see Figure 3-2). In order to locate these points, it is first necessary to determine if the inner quadrangle, defined by points P1 P2 P3 P4 in that order, progresses in a clockwise or counterclockwise direction (the reason for this is discussed in the next section). If the progression from P1 to P2 to P3 to P4 is clockwise, then the cross-products of the sides of the inner quadrangle will be negative. If counterclockwise, then the cross-products will be positive. The cross products discussed here are as follows:  $\underline{S1} \times \underline{S2}$ ,  $\underline{S2} \times \underline{S3}$ ,  $\underline{S3} \times \underline{S4}$ , and  $\underline{S4} \times \underline{S1}$ , and are obtained as described in Section 3-1.3.

As an example for this procedure, we consider Figures 3-3 and 3-4. In Figure 3-3, we have assumed for example that the inner quadrangle progression P1 P2 P3 P4 is clockwise. We know the locations of P1 and P2 and it is apparent that the polygon P1 P12 P21 P2 is a rectangle. Therefore, the slope of line SR1 is the negative inverse of the slope (SM1) of line S1. We can therefore write 2 equations:

$$YR1 / XR1 = -1./SM1$$
$$YR1^2 + XR1^2 = SR1^2 \quad \text{Where } SR1 = R \text{ in magnitude}$$

Solving these simultaneously:

$$X12 = X1 - FX * R$$

$$Y12 = Y1 + FY * R$$

where  $FX = 1./SQRT(1. + 1./SM1 ** 2)$   
 $FY = 1./SQRT(1. + SM1 ** 2)$

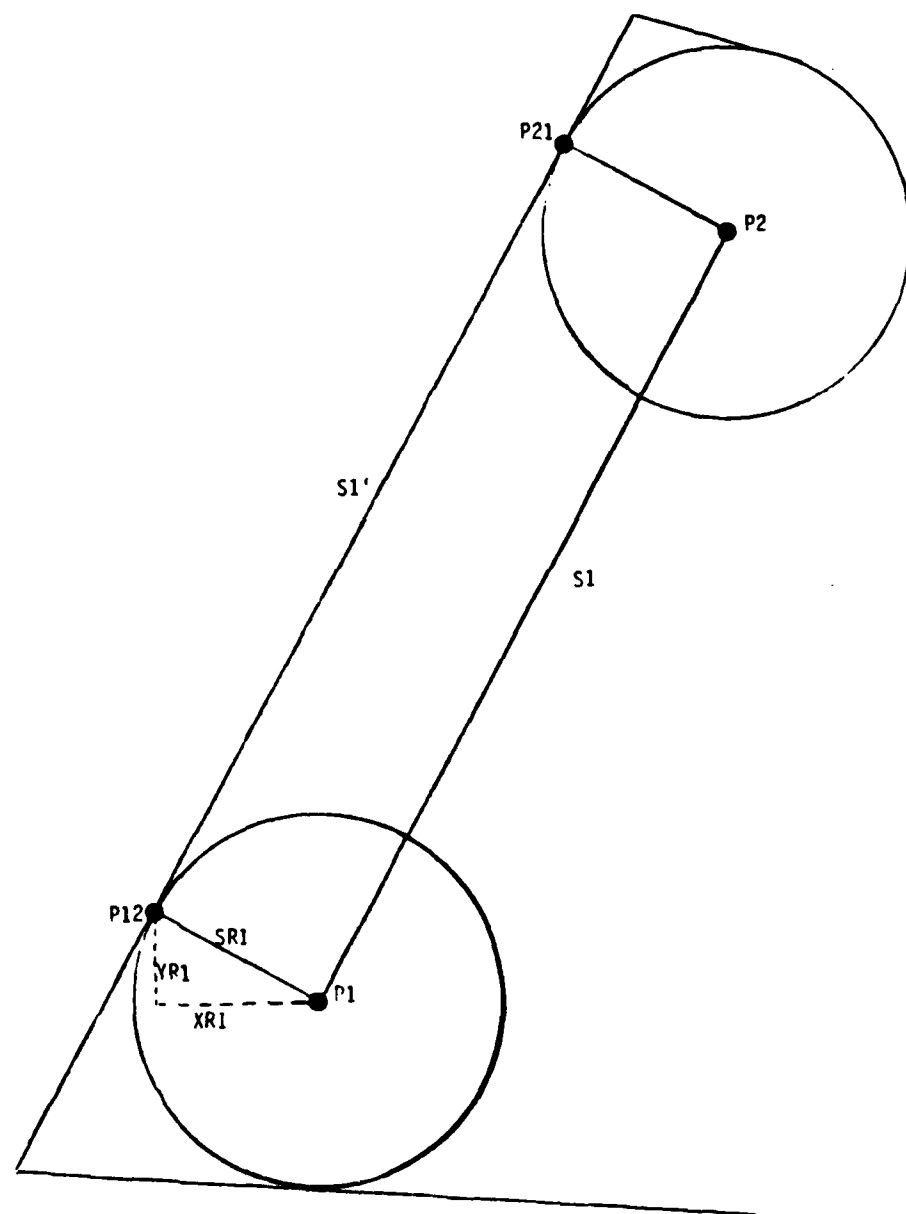


Figure 3-3. Detail for finding the tangent points P11, P12, P21, P22, P31, P32, P41, P42.

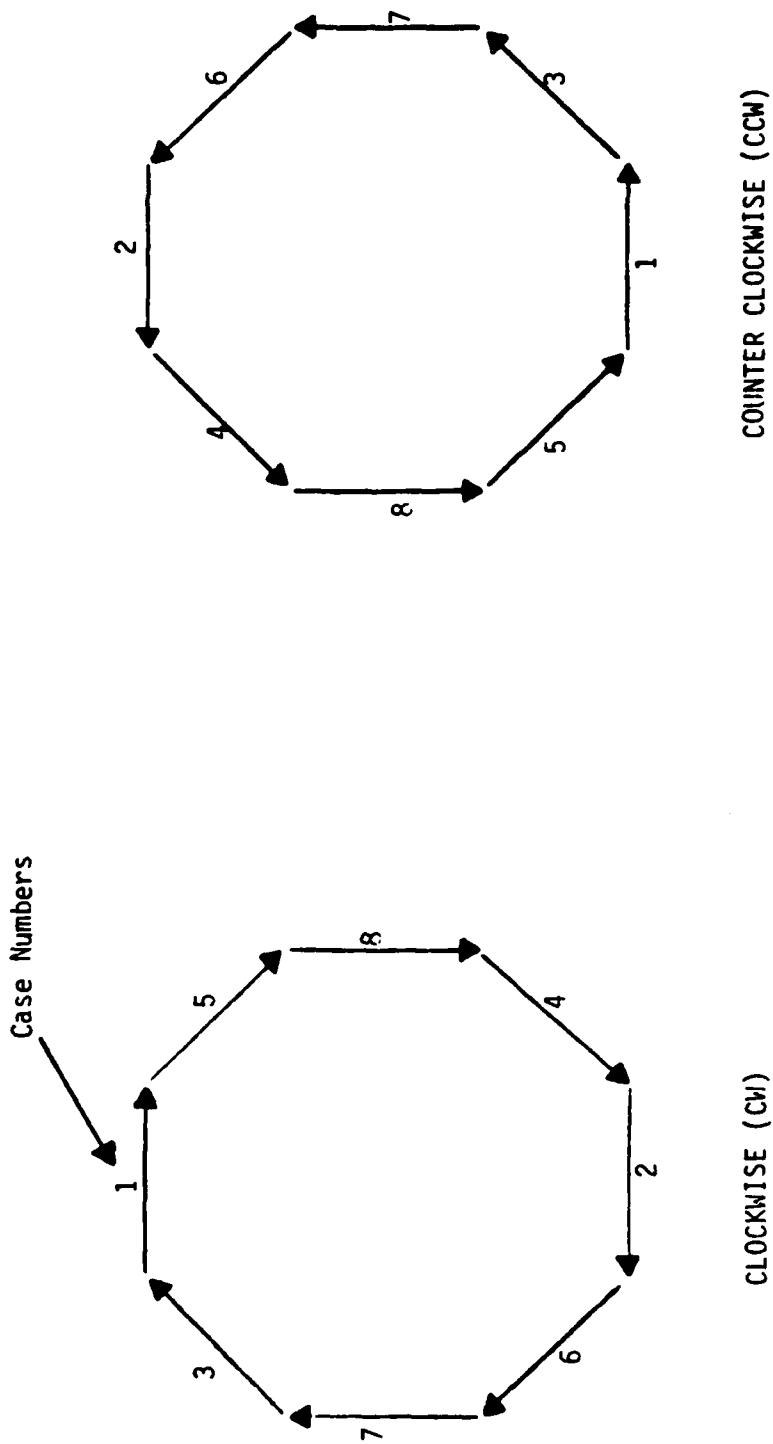


Figure 3-4. Possible orientations of quadrangle sides  $S1'$ ,  $S2'$ ,  $S3'$ ,  $S4'$ .

This particular example has been case 3 of the clockwise case. To understand its context in the overall calculation, and the other equations involved, consider Figure 3-4 and Table 3-1. Figure 3-4 shows the various possible orientations of the lines  $S_1$  (hence  $S_1'$ ),  $S_2$  (hence  $S_2'$ ),  $S_3$  (hence  $S_3'$ ), and  $S_4$  (hence  $S_4'$ ) along with the corresponding "case numbers". Table 3-1 shows the resulting equations for the X and Y locations of the points  $P_{12}$  and  $P_{21}$  for each case in both the clockwise and counterclockwise conditions. We can see from Figures 3-3 and 3-4 and Table 3-1 the necessity of knowing the clockwise/counterclockwise condition (hence the cross-product signs). For the CCW case, the tangent points all lie to the right of the points  $P_1, P_2, P_3, P_4$ . For the CW case, they all lie to the left.

### 3-1.5 Finding the Outer Quadrangle Vertices $P_{13}, P_{23}, P_{33}, P_{43}$

The procedure for finding these points is to find the general equations for the lines  $S_1', S_2', S_3',$  and  $S_4'$  and solve each intersecting pair simultaneously to locate the point of intersection. The general form of the equation of a line is:

$$AX + BY + C = 0$$

Let us look at the particular point  $P_{13}$ , and the equations that will lead to its location. The slopes of the lines  $S_1'$  and  $S_4'$  are equal to those of  $S_1$  and  $S_4$ ; i.e.,  $SM_1$  and  $SM_4$ . We can therefore write:

$$Y - Y_{12} = SM_1 * (X - X_{12})$$

$$Y - Y_{42} = SM_4 * (X - X_{42})$$

rearranging to get the general form, we get:

$$Y - SM_1 * X + (SM_1 * X_{12} - Y_{12}) = 0$$

$$Y - SM_4 * X + (SM_4 * X_{42} - Y_{42}) = 0$$

solving for X:

$$X_{13}(IB, IA) = (X_{42} * SM_4 - X_{12} * SM_1 + Y_{12} - Y_{42}) / (SM_4 - SM_1)$$

**Table 3-1. Equations for the tangent points P12, P21 for all orientations of S1  
(equations for other tangent points are analogous for other lines S2, S3, S4).**

<u>Case Number</u>	<u>Slope SM1</u>	<u>X2-X1 = DX1</u>	<u>CW Equations</u>	<u>CCW Equations</u>
1	0	.GT.0	X12=X1 Y12=Y1+R X21=X2 Y21=Y2+R	X12=X1 Y12=Y1-R X21=X2 Y21=Y2-R
2	0	.LT.0	X12=X1 Y12=Y1-R X21=X2 Y21=Y2-R	X12=X1 Y12=Y1+R X21=X2 Y21=Y2+R
3	.GT.0	.GT.0	X12=X1-FX*R Y12=Y1+FY*R X21=X2-FX*R Y21=Y2+FX*R	X12=X1+FX*R Y12=Y1-FY*R X21=X2+FX*R Y21=Y2-FY*R
4	.GT.0	.LT.0	X12=X1+FX*R Y12=Y1-FY*R X21=X2+FX*R Y21=Y2+FY*R	X12=X1-FX*R Y12=Y1+FY*R X21=X2-FX*R Y21=Y2+FY*R
5	.LT.0	.GT.0	X12=X1+FX*R Y12=Y1+FY*R X21=X2+FX*R Y21=Y2+FY*R	X12=X1-FX*R Y12=Y1-FY*R X21=X2-FX*R Y21=Y2-FY*R
6	.LT.0	.LT.0	X12=X1-FX*R Y12=Y1-FY*R X21=X2-FX*R Y21=Y2-FY*R	X12=X1+FX*R Y12=Y1+FY*R X21=X2+FX*R Y21=Y2+FY*R
7	$\infty$	DY1.GT.0	X12=X1-R Y12=Y1 X21=X2-R Y21=Y2	X12=X1+R Y12=Y1 X21=X2+R Y21=Y2
8	$\infty$	DY1.L.T.0	X12=X1+R Y12=Y1 X21=X2+R Y21=Y2	X12=X1-R Y12=Y1 X21=X2-R Y21=Y2

If we solve for Y, we get:

$$Y_{13}(IB, IA) = (Y_{12} \cdot SM4 - Y_{42} \cdot SM1 + (X_{42} - X_{12}) \cdot SM4 \cdot SM1) / (SM4 - SM1)$$

The equations for P23, P33, and P43 are obtained through the same method.

### 3-1.6 Finding the Total Area of Activity Spread

The total area over which the activity from disc (IB, IA) is spread can be calculated by considering it to consist of three parts (see Figure 3-2):

- The area of the "inner" quadrangle P1, P2, P3, P4 (AREA  $\emptyset$  in Subroutine SMEAR).

This area is obtained from the expression for the area of a polygon from analytic geometry, and is:

$$\begin{aligned} \text{AREA } \emptyset (IB, IA) = & 0.5 * (X_1 * Y_2 + X_2 * Y_3 + X_3 * Y_4 + X_4 * Y_1 \\ & - X_2 * Y_1 - X_3 * Y_2 - X_4 * Y_3 - X_1 * Y_4) \end{aligned}$$

where all the points in the parentheses are subscripted (IB, IA).

- The areas of the 4 quadrangles (P1, P2, P21, P12), (P2, P3, P31, P22), (P3, P4, P41, P32), and (P4, P1, P11, P42). The total of these 4 areas is equal to  $R * (S1 + S2 + S3 + S4)$ .
- The remaining 4 areas from the corner discs (e.g., P21-P2-P22-P21). It can be shown that, regardless of the relative orientations of the points P1, P2, P3, P4, these 4 areas total up to  $\pi R^2$ .

### 3-1.7 A Word About the Quadrangle Corners

The SMEAR theory considers a spread of extremely thin discs across the area described above, each representing an extremely small increment of altitude and particle size. The extremities of the area spread will be the corner discs, and do not include the corners (the shaded portion in Figure 3-5). However, the method of determining if map points are within the area (Subroutine MAPDEN discussed in Section 4.3) is such that map points that lie within the shaded area will be counted unless otherwise excluded. Such an exclusion routine is incorporated in Subroutine SMEAR.

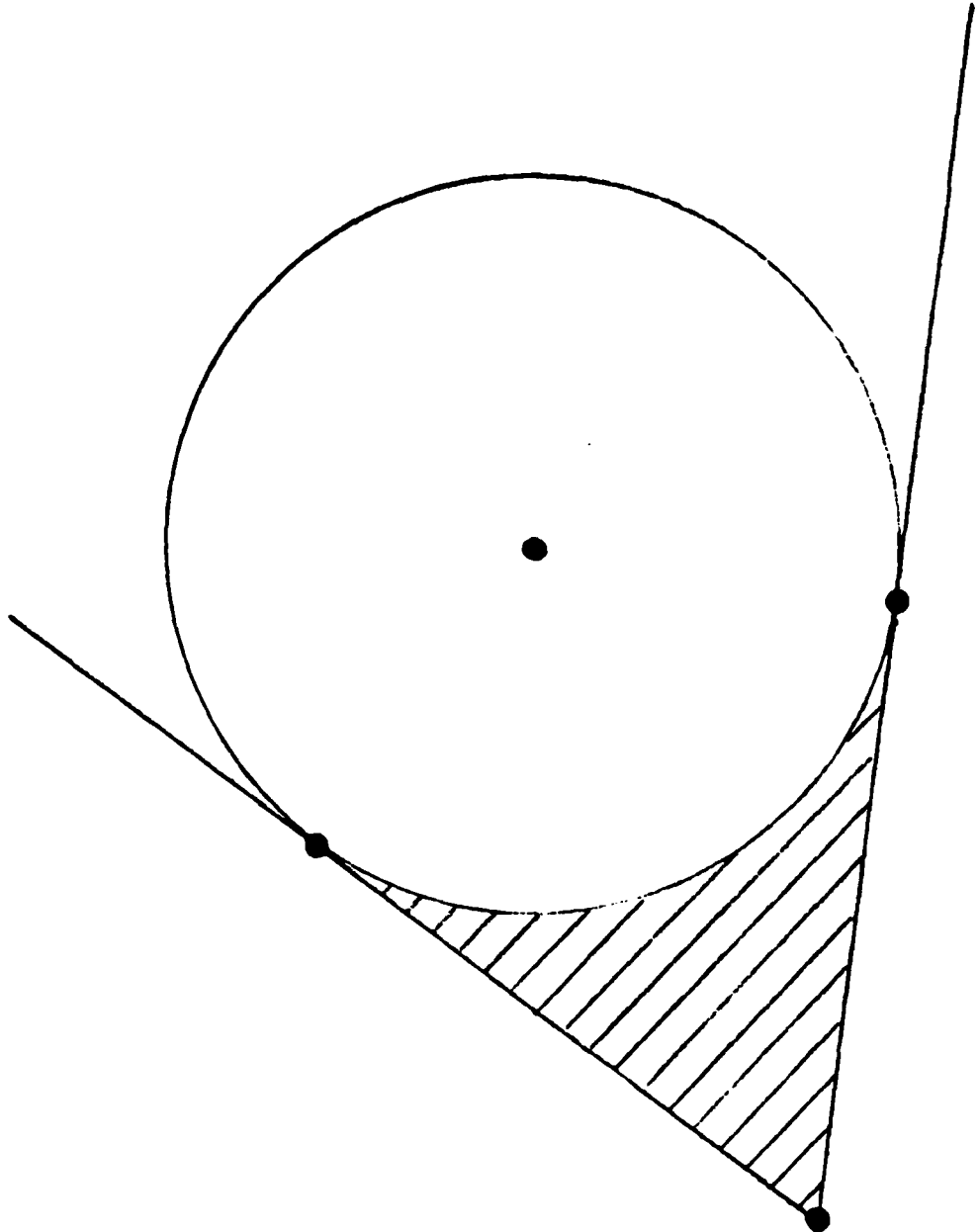


Figure 3-5. Illustration of corner areas excluded in activity spread.

### 3-1.8 Computing the Fallout Activity Density

The total fallout activity input to the modified SEER can be in terms of curies/KT at 1 hour, or R/hr at 1 hour 3 ft above an infinite plane, or some other value (represented by SEED) input by the user. The activity in each altitude slab of the stabilized cloud is:

$$\text{ACTLYR} = \text{SEED} * \text{YLD} * \text{FFR} * \text{PCT} / \text{FLOAT (NSLABS)}$$

where

YLD = yield in KT, and PCT and FFR are correction factors already in SEER.

The activity density in the quadrangle is thus

$$\text{DENS (IB,IA)} = \text{ACTLYR} * \text{PERCNT (IB) / AREA (IB,IA)}$$

where PERCNT (IB) is the percent of total activity ascribed to the particular IB<sup>th</sup> particle size group.

### 3-2 SETTING UP THE FALLOUT MAP (SUBROUTINE GRID)

The purpose in establishing the map grid at this point is that the methodology used in subroutine MAPDEN (description below) requires that the coordinates of the map points be known. This is in contrast with the current SEER method, which computes activity densities at "key points" before the grid is established, and later computes the activity densities at the map points by interpolation between the key points. The map points established in GRID are all located in terms of X and Y distances in meters from GZ. The basic approach to map construction is the same as SEER. That is, the map is printed on a line printer with X-values increasing from left-to-right and y-values printed in decreasing order from top-to-bottom. The Y-length may be as long as the user wishes (AMGY), and the X-width may be divided into strips so that the printer can handle a wide map that still retains some reasonable resolution. The user puts in the number of X points (NCOL) to be used for each strip, and also puts in an estimate of the total number of X points (AMGX) required, usually some multiple of NCOL. An alternate method is available by setting an index (IMAP) to 1. This allows the user to input the extent of the map in both the X and Y directions, and also the distance (DEL) from one grid point to the

next (DEL is the same in the X and Y directions). This feature duplicates a feature that is available in DELFIC, and is particularly useful if one has an idea of the extent of activity levels of interest (say from a prior execution of SEER) that would thus allow the map routine to avoid calculations over extended areas of low activity. The use of this feature allows the program to skip over the calculations described in the next two subsections.

### **3-2.1 Finding the Max/Min Limits of the Fallout Distribution**

This is achieved by finding the maximum and minimum values of X and Y for the quadrangle vertices for all IA levels and IB particle size groups. The extreme values found for each are called XMIN, XMAX, YMIN, YMAX.

### **3-2.2 Setting up the Grid**

A grid is set up as follows: First the extents of fallout in the X and Y directions are determined

$$\text{DELX} = \text{XMAX} - \text{XMIN}$$

$$\text{DELY} = \text{YMAX} - \text{YMIN}$$

Next, the grid increment is determined. A square grid increment is used; that is, the increment (DEL) from one X-point to the next is the same as that from one Y-point to the next. The following quantities are computed:

$$F1 = \text{DELX/AMGX}$$

$$F2 = \text{DELY/AMGY}$$

and the quantity  $F3 = \text{AMAX1}(F1, F2)$  is taken as the first approximation to DEL. F3 is then increased slightly up to some multiple of 10, 100, 1000, etc (this makes the map easier to read than the current SEER). The map starting points are established at some X value just less than XMIN that is divisible by DEL, and some Y-value just greater than YMAX which is divisible by DEL. The number of X-points in the map is calculated as

$$\text{NXPTS} = \text{IFIX}(\text{DELX/DEL}) + 3$$

where 3 has been added to correct for truncation and to provide a margin on either side of the map. The number of Y points is determined in a similar manner. The number of map strips required is determined by comparing NXPTS with NCOL.

### **3-3 CALCULATING THE FALLOUT ACTIVITY DENSITY AT EACH MAP POINT (SUB-ROUTINE MAPDEN)**

MAPDEN loops through each disc AREA (IB,IA) (IA=1, NSLABS), (IB=1, 25) to determine which map points fall within the area. This could require excessive computer time if each IA,IB iteration had to consider all of the map points. In order to save time, the number of map points can be limited to those that are in the near vicinity of the quadrangle because the map grid point locations have already been established in Subroutine GRID.

#### **3-3.1 Find the Limit "Box" for Map Points**

The limits for map points to be considered are established by a rectangle with sides parallel to the X and Y axes and X, Y values of:

$$X_{MAX} = AMAX1 (X_{13}, X_{23}, X_{33}, X_{43})$$

$$X_{MIN} = AMIN1 (X_{13}, X_{23}, X_{33}, X_{43})$$

$$Y_{MAX} = AMAX1 (Y_{13}, Y_{23}, Y_{33}, Y_{43})$$

$$Y_{MIN} = AMIN1 (Y_{13}, Y_{23}, Y_{33}, Y_{43})$$

where all the values in parentheses are subscripted (IB, IA). The map point subscript limits are then established as IMIN, IMAX, JMIN, JMAX.

#### **3-3.2 Check Each Map Point in the "Limit Box" to See if it Falls in the Area**

The approach used here is the one used by computer graphics routines to determine whether a line or point is "masked" by another surface. The signs of the cross-products of each of the four sides of the quadrangle with the next side  $\underline{S1'xS2'}$ ,  $\underline{S2'xS3'}$ ,  $\underline{S3'xS4'}$ , and  $\underline{S4'xS1'}$  are compared with the signs of the cross-products of each side cross the vector between the appropriate quadrangle vertex and the map point in question. This is illustrated in Figure 3-6, where the sign of  $\underline{S1'xS2'}$  is the same as that of  $\underline{S1'xMP1}$  (where map point MP1 lies in the quadrangle) and is not the same as

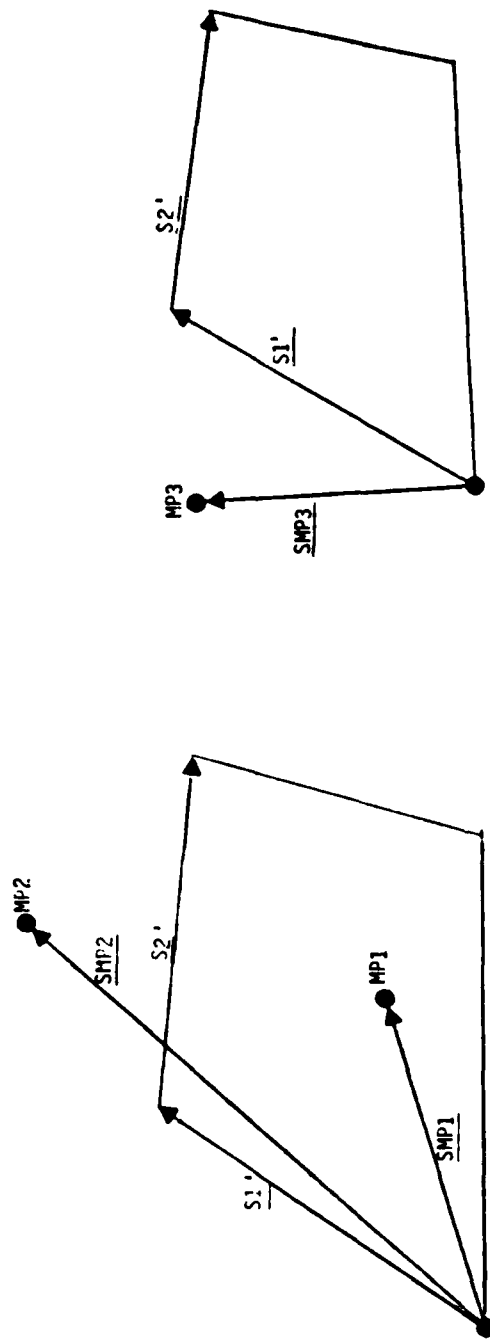


Figure 3-6. Illustration of cross-product method of determining if a map point is within quadrangle area.

S1'xSMP3 (which lies outside the quadrangle). However, the sign is the same as that of S1'xSMP2 where MP2 lies outside the quadrangle. Therefore, the signs of all four sides must be checked before a map point can be counted "in" the quadrangle. However, the map point can be counted "out" of the quadrangle at the first case of disagreement of sign. As stated before, an additional check is made to exclude points that lie in the "corners" of the quadrangle.

### 3-3.3 Increase Activity Density of Map Point

If the cross-products have agreed in sign in all 4 cases, we can increase the activity density of the map point I, J by that of the IB,IA quadrangle:

$$\text{DENSMP}(I,J) = \text{DENSMP}(I,J) + \text{DENS}(IB,IA)$$

### 3-3.4 Check for Rough Agreement of Total Fallout Activity

A check can be made for approximate agreement between the known total fallout activity and the following quantity:

$$\text{TOTACT} = \text{TOTDEN} * \text{DEL} * \text{DEL}$$

where  $\text{TOTDEN} = \sum_{\text{all } ij} \text{DENSMP}(I,J)$

This should not necessarily be expected to yield close agreement since the value of  $\text{DENSMP}(I,J)$  is not necessarily uniform across its  $(I,J)^{\text{th}}$  incremental area.

## 3-4 PLOTTING THE MAP (SUBROUTINE PLTMAP)

This routine simplifies the plotting procedures used in SEER because it is no longer necessary to plot shoulders, edges, a separate GZ area, or do interpolations. The SEER map procedure has also been changed to plot dots and blanks where no activity occurs, as does the DELFIC map routine. The current SEER routine (CATALG) plots zeros, and is therefore more difficult to read. A print of X and Y coordinate values across the top and down the right side of the map has also been added. The value of TOTACT is printed at the map bottom, but the same caveat applies as discussed in Section 3-3.4.

### 3-5 SUMMARY OF SUBROUTINES ADDED AND REPLACED

Subroutines added and replaced are:

<u>Subroutines Added by Modified Approach</u>	<u>Current SEER Subroutines Replaced (not used) in Modified Approach</u>	
RTLFT	SEER 3	CROSS
SMEAR	SEER 4	DNWD5
GRID	SEER 5	DOSMP
MAPDEN	FODOSE	INTP5
PLTMAP	CATALG	EANDF5
	DOWN5	EDGY5
	EDGE5	SHLD5
	GRDZ5	UPWD5
	CIRC5	

### 3-6 NEW PARTICLE SIZE GROUP ACTIVITY DISTRIBUTION

For this comparison effort, SEER was modified to provide the user with the capability of selecting a particle size group activity distribution which approximates that currently used in DELFIC. The latter was obtained by modifying DELFIC slightly (at GXPSR.61) to print out the percentage of activity of each of its 100 particle size classes. These percentages were grouped into 25 classes to coincide as much as possible with the sizes of the 25 SEER size classes. The user can select this new particle size group activity distribution or the one currently in SEER by the input of the value 3 (new) or 1 (current) for the index KPGS.

## SECTION 4

### COMPARISON RESULTS

The comparisons made to judge the relative effectiveness of the two versions of SEER were done in two phases. The first phase was done for just one wind and served to establish the validity of the new SEER methodology. The current SEER version used did not have the adjusted K-factor, and thus was essentially not the version of SEER currently used in CIVIC. The phase one comparison thus only establishes the improvement of SEER over the pre-CIVIC version. The phase two comparison included the current CIVIC version of SEER with adjusted K-factor, and was done for the multiple hypothetical cases (two yields, eleven winds) that were treated in References 1 and 5.

#### 4-1 PHASE ONE RESULTS - COMPARISON WITH PRE-CIVIC SEER

The pre-CIVIC version of SEER (NEW = 0), the modified SEER (NEW = 1), and DELFIC were run for the case of a 1.0 MT surface burst and the winds observed at 0630 25 Dec. 1971 at Templehof Airport, Berlin, Germany. Both SEER cases (NEW = 0 and NEW = 1) were run with the existing SEER particle size group activity distribution, as well as with an activity distribution which approximates that of DELFIC (see Section 3-6).

##### 4-1.1 Comparisons of Activity Areas, Integrated Activity, Run Times

Table 4-1 summarizes the results obtained from running DELFIC and the two versions of SEER, each with the two particle size class activity assignments, KPGS = 1 and KPGS = 3. The following comments should be noted in regard to these results:

- The areas enclosed in the activity contours were obtained in all cases simply by multiplying the number of map points whose activity exceeded the particular level, by the incremental area represented by each map point (53.3 km<sup>2</sup> for DELFIC, 103.3 km<sup>2</sup> for SEER (NEW = 0), and 64.0 km<sup>2</sup> for SEER (NEW = 1)).

Table 4-1. Summary of results from DELFIC and SEER.

	SEER (NEW, KPGS)*			
	<u>DELFIC</u>	<u>0, 1</u>	<u>0, 3</u>	<u>1, 1</u>
<b>Areas (in km<sup>2</sup>) Enclosed Within Activity Contours (r/hr @ 1 hr.)</b>				
10	43,150	73,680	74,190	50,050
100	6,133	9,403	8,370	7,552
1000	480	1,343	826	704
3000	53	310	103	0
<b>Integrated Activity (10<sup>12</sup> r/hr @ 1 hr)</b>				
	4.014	6.796	5.823	4.346
				3.700
<b>Farthest Extent of Contour from GZ (km)</b>				
10	709	705	713	725
100	201	255	275	215
1000	48	73	65	56
3000	11	27	25	--
<b>Run Time (sec)</b>	<b>41.666</b>	<b>0.654</b>	<b>0.689</b>	<b>0.845</b>
				<b>0.819</b>

- \* NEW = 0: Existing version of SEER before modification
- NEW = 1: SEER modified to conserve activity
- KPGS = 1: Particle size class activity assignment currently in SEER
- KPGS = 3: Particle size class activity assignment from DELFIC

- The integrated activity was obtained by multiplying the map point activity value by the incremental area represented by each map point. Since the activity is not uniform from one map point to the next, the values are not expected to have a high degree of precision.
- The extent of the integrated activity summation was over just the area of the fallout field that was plotted, and did not include outlying areas of low activity. Thus, the total value should be expected to be less than the fallout portion of the total activity within the cloud. Fallout activity values are discussed below in Section 4-1.3.
- The furthest extent from the GZ of the 4 contour areas is a program output in the DELFIC program, and those values are the ones shown. The values for SEER are measured from the output maps. No values for 3000 R/HR are given for SEER (NEW = 1) because that activity value was not obtained for any of the map points.

#### 4-1.2 Contour Plot Comparisons

Figures 4-1 through 4-11 show comparative plots of activity contours for 10, 100, 1000, and 3000 r/hr (at 1 hour after detonation). In each figure, the DELFIC contour is compared to one of the 4 SEER cases ((NEW, KPGS) = (0, 1), (0, 3), (1, 1), (1, 3)) (see note at bottom of Table 4-1), except that no plot is shown for the 10 r/hr case for (0, 3) because it does not look significantly different than (0, 1). The maps plotted in this comparison for SEER1 had map points spaced 8 km apart.

#### 4-1.3 A Word About Fallout Activity

DELFIC does not use a K-factor, or initialized value of total activity, in order to set the level of fallout activity (p. 26 of Ref. 4, p. 8 of Ref. 8).\* A fast-running code to approximate DELFIC, such as SEER, must therefore start with some initial total activity level obtained from the literature. Table 4-2 shows values provided in the indicated references. As can be seen, there is some disparity among the values reported. Moreover, there must also be an adjustment for the percent of total activity that is deposited in the so-called "early fallout." This early fallout is the only part that is of strategic significance in the calculations to be made with SEER, and this fraction must therefore be multiplied by the total activity to obtain the "K-factor." The current SEER uses a K-factor of  $6.0775 \times 10^9$  (r/hr)/(KT/m<sup>2</sup>), which

---

\*However, Reference 10 describes a modification to DELFIC to allow use of a K-factor in a conventional activity calculation.

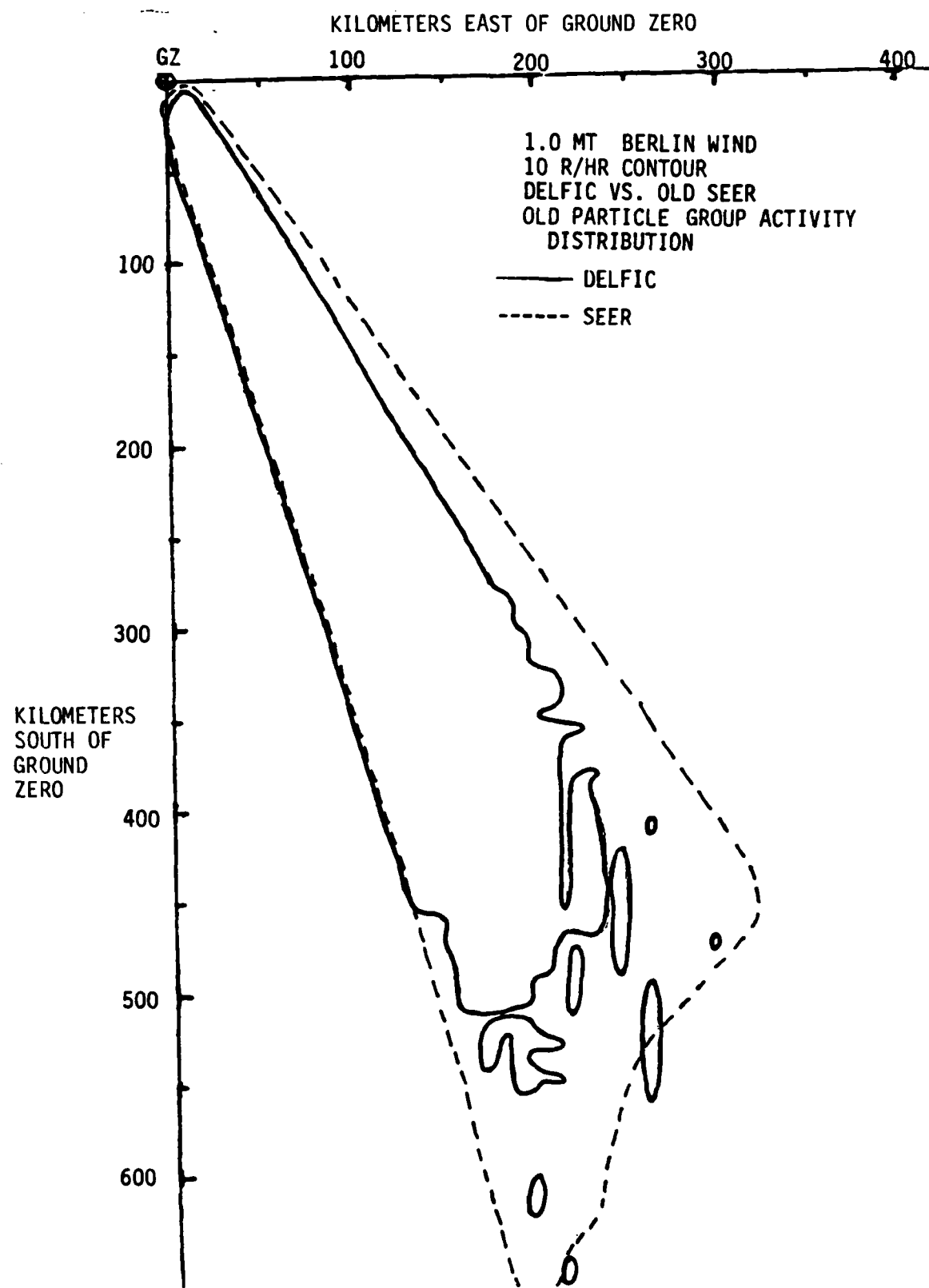


Figure 4-1. 10 r/hr contour, DELFIC vs. old SEER.

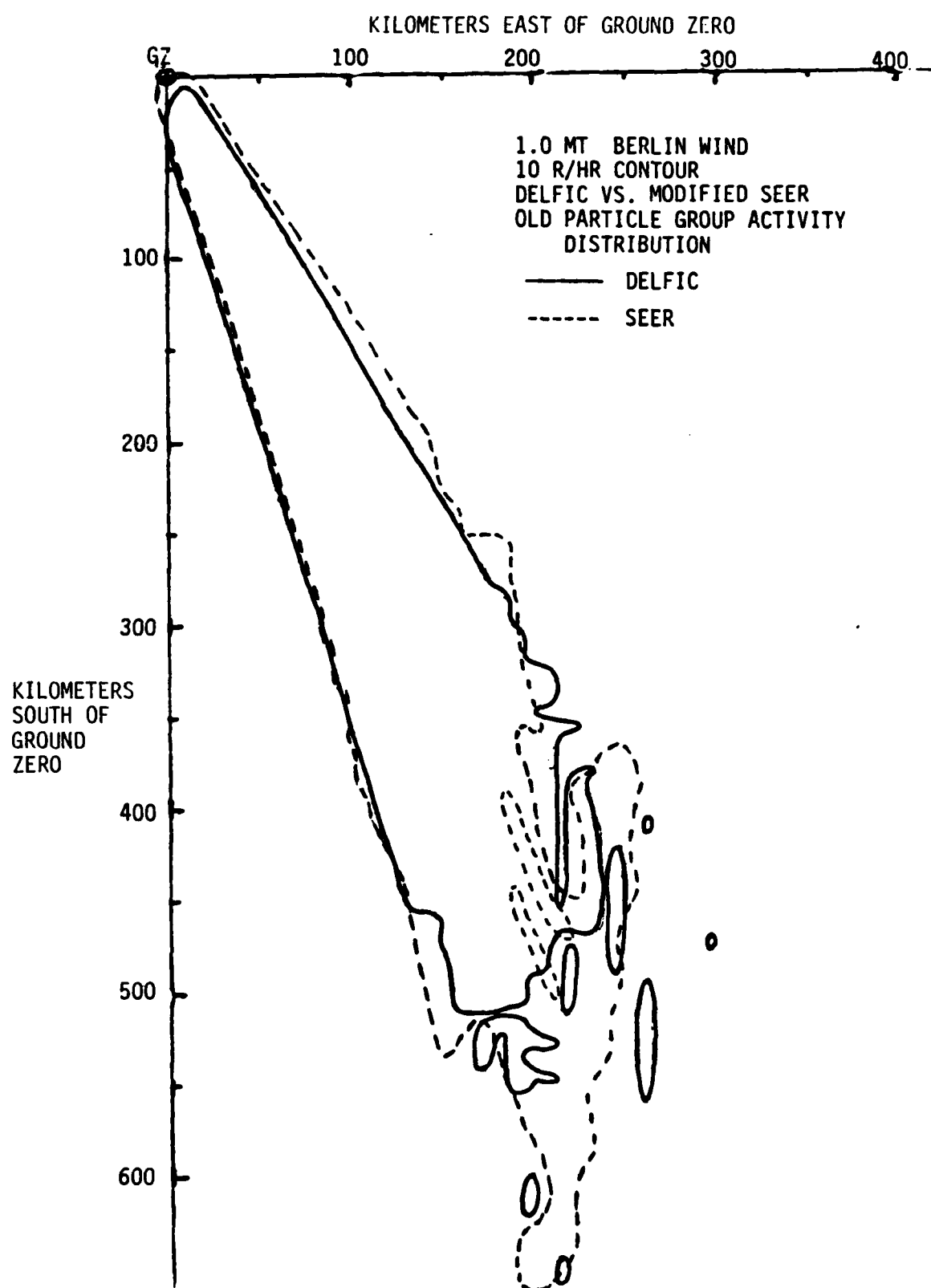


Figure 4-2. 10 r/hr contour, DELFIC vs. modified SEER.

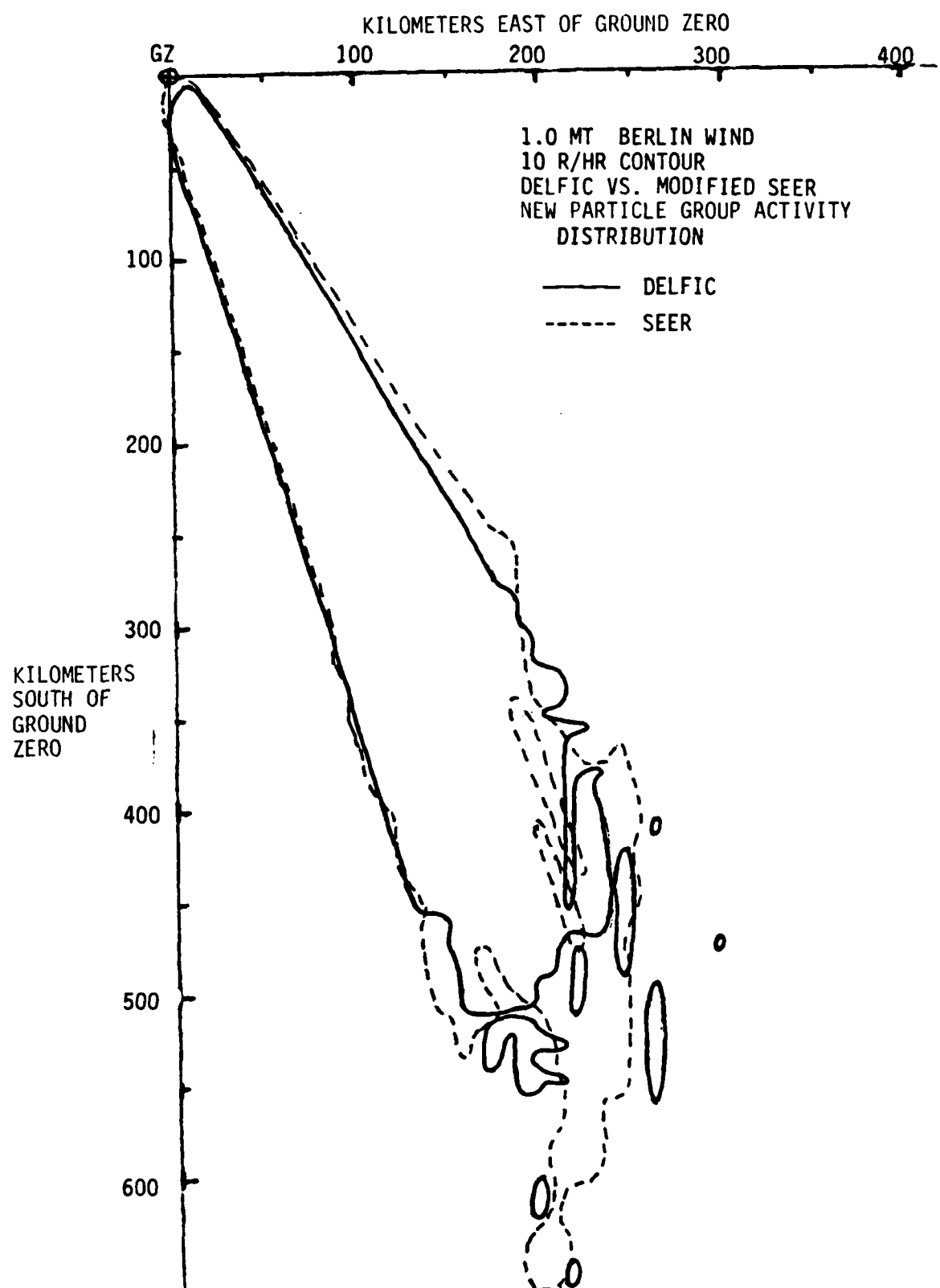


Figure 4-3. 10 r/hr contour, DELFIC vs. modified SEER, new activity distribution.

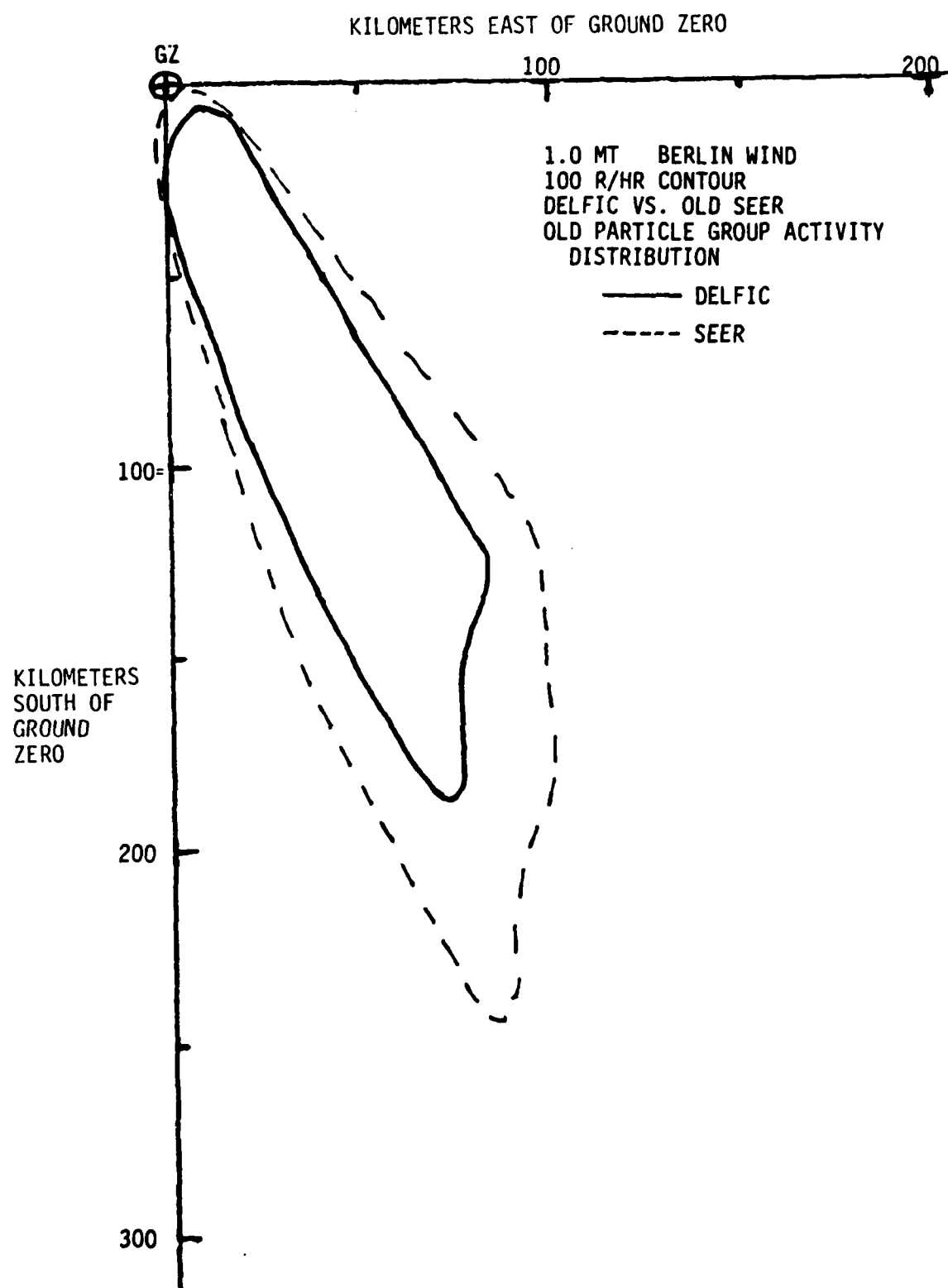


Figure 4-4. 100 r/hr contour, DELFIC vs. old SEER.

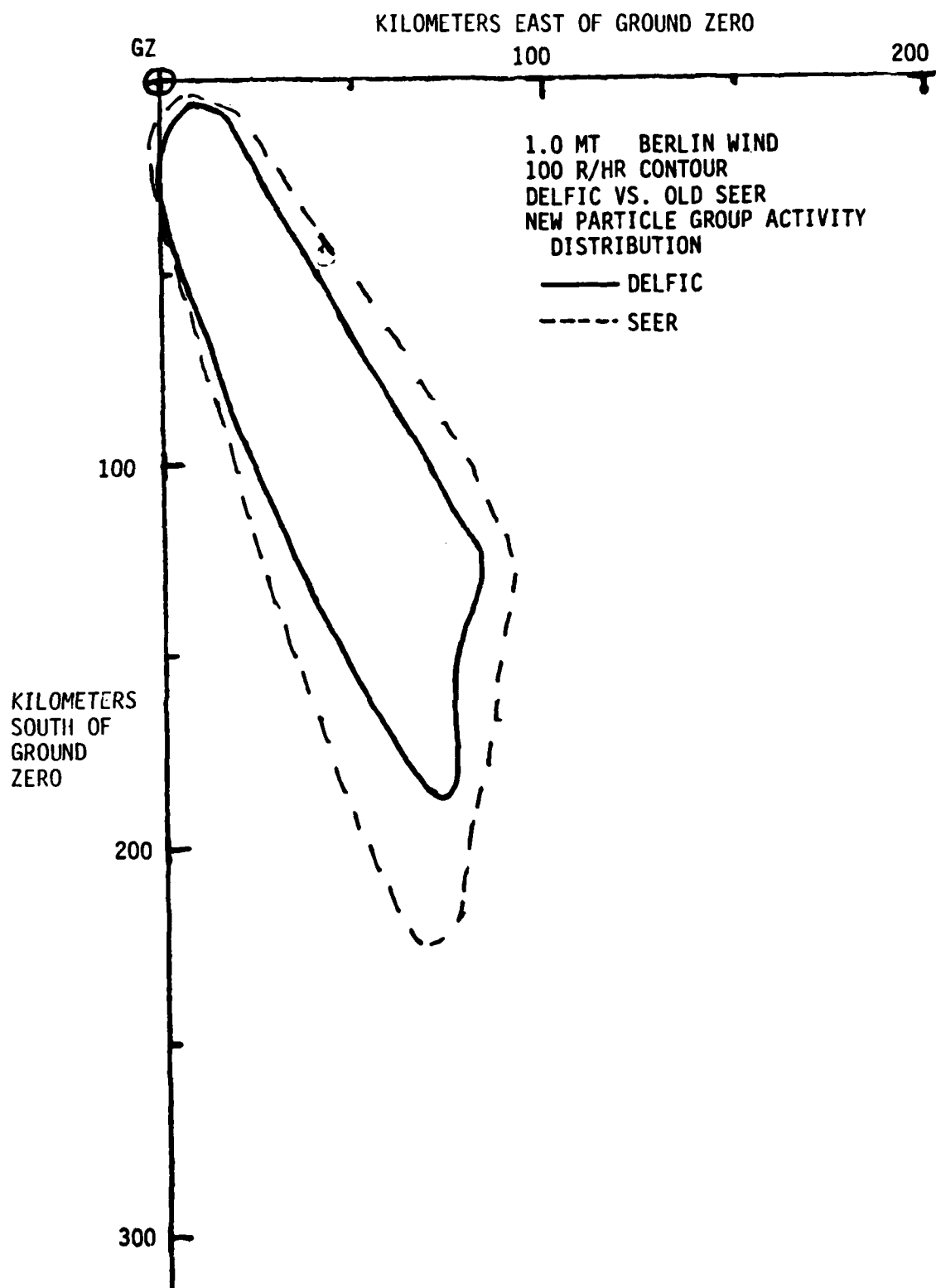
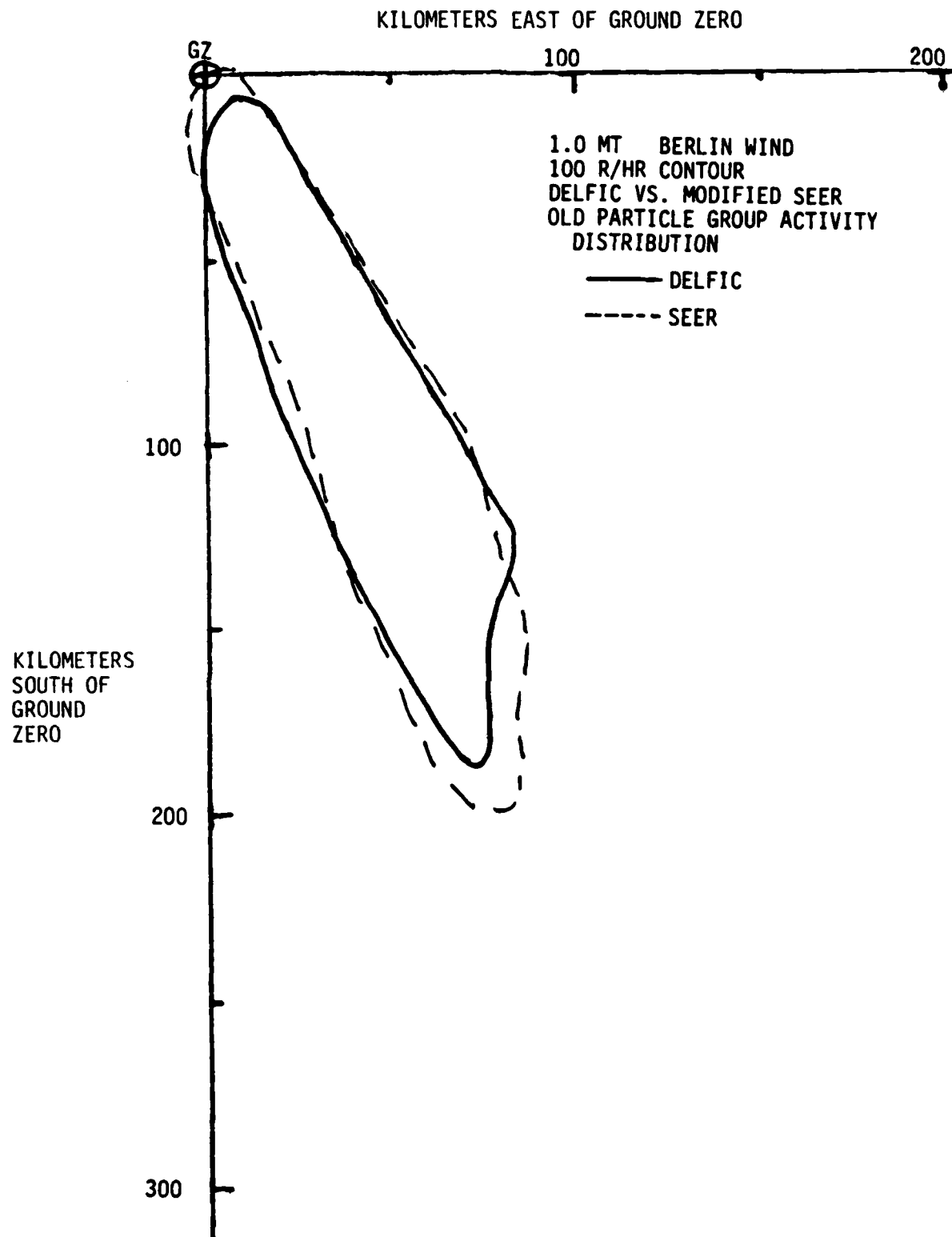


Figure 4-5. 100 r/hr contour, DELFIC vs. old SEER, new activity distribution.



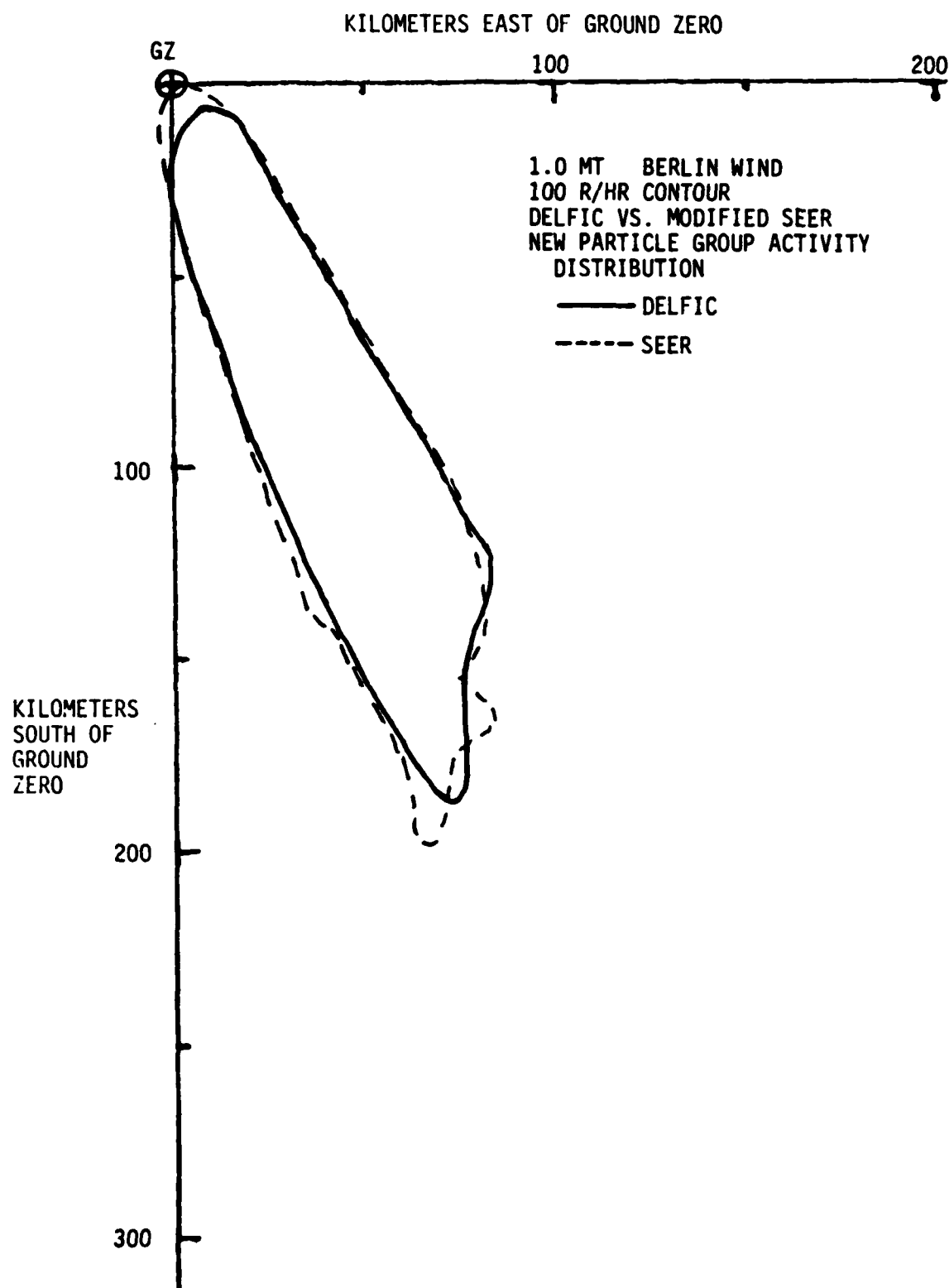


Figure 4-7. 100 r/hr contour, DELFIC vs. modified SEER, new activity distribution.

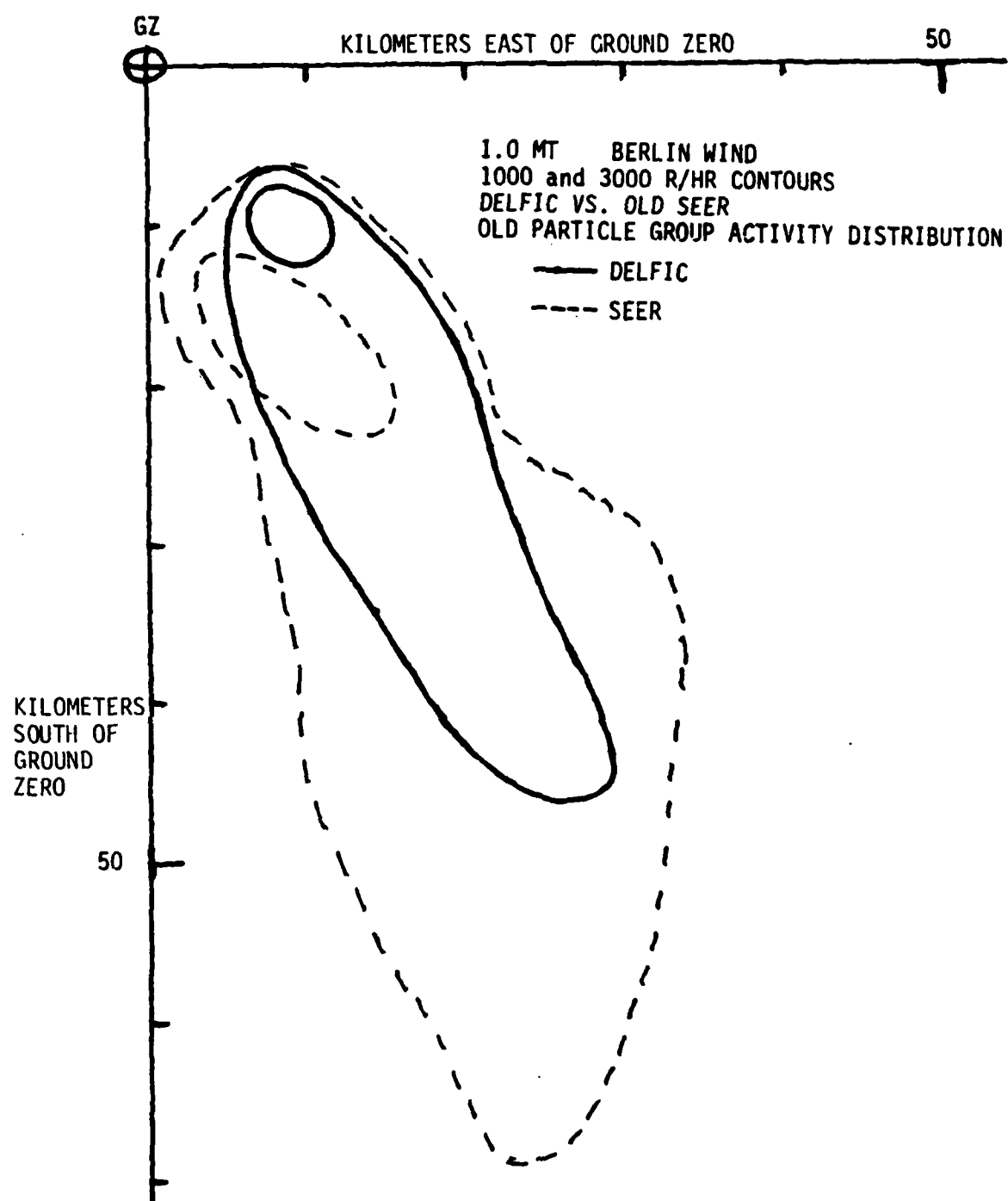


Figure 4-8. 1000 and 3000 r/hr contours, DELFIC vs. old SEER.

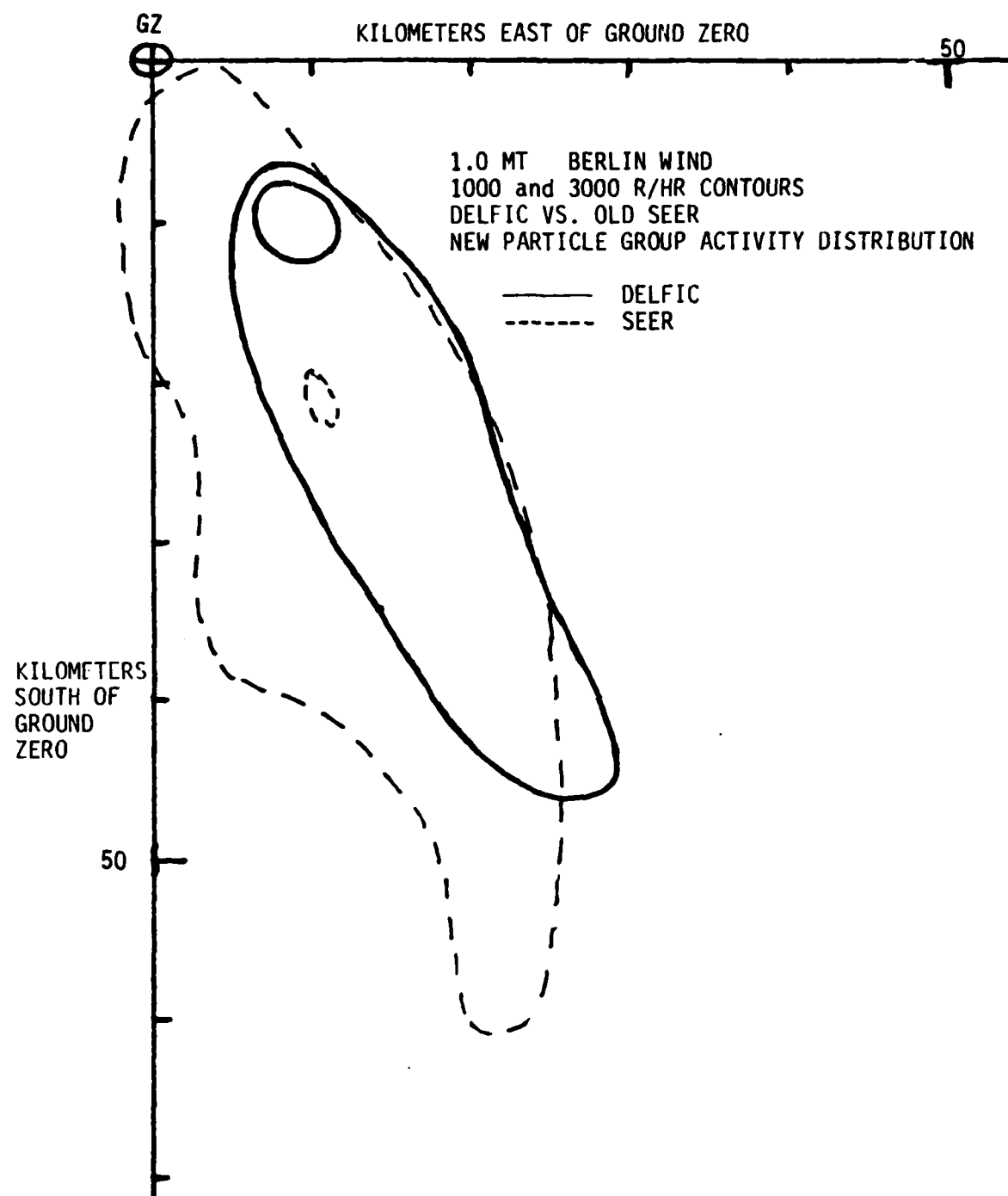


Figure 4-9. 1000 and 3000 r/hr contours, DELFIC vs. old SEER, new activity distribution.

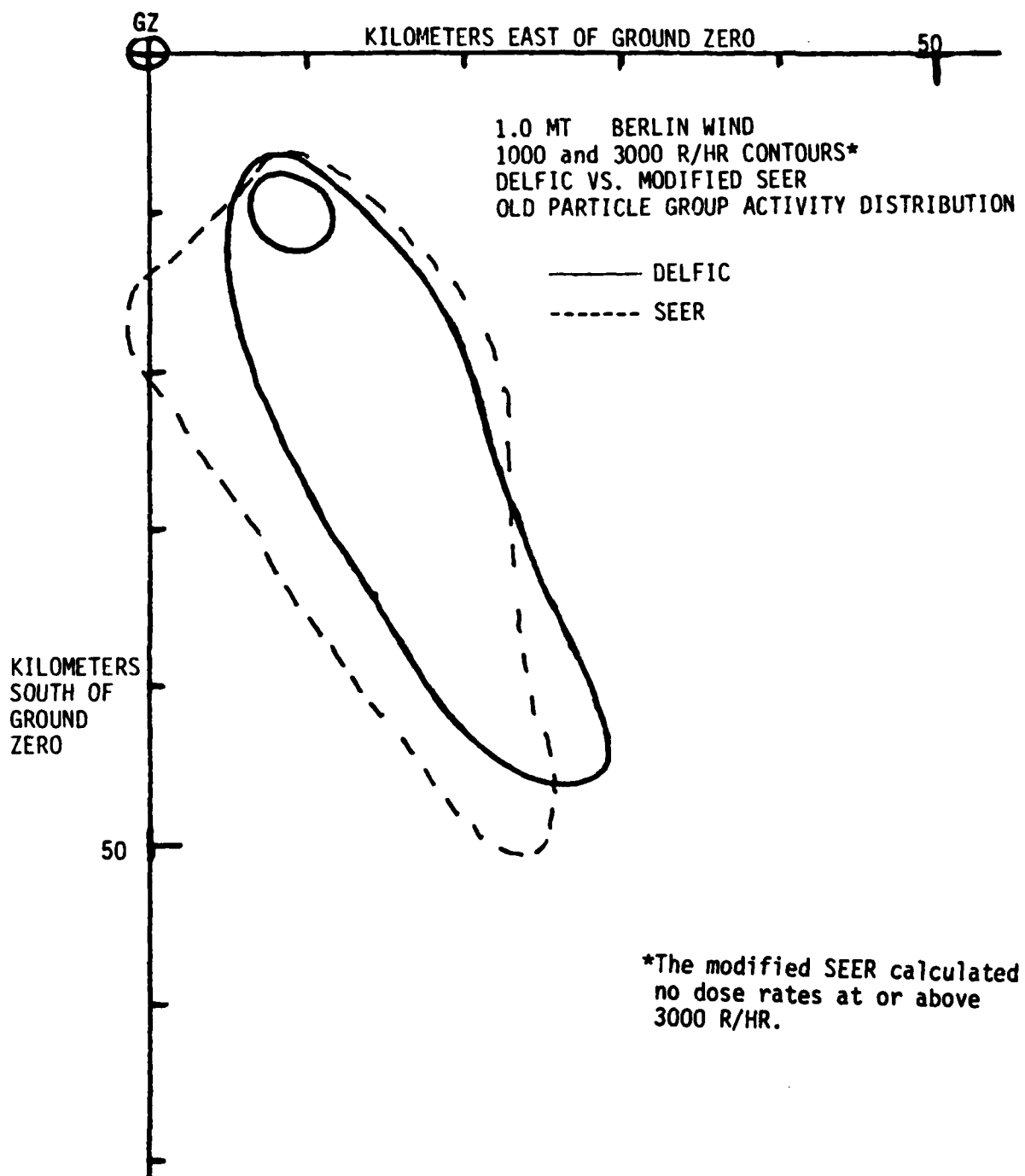


Figure 4-10. 1000 and 3000 r/hr contours, DELFIC vs. modified SEER.

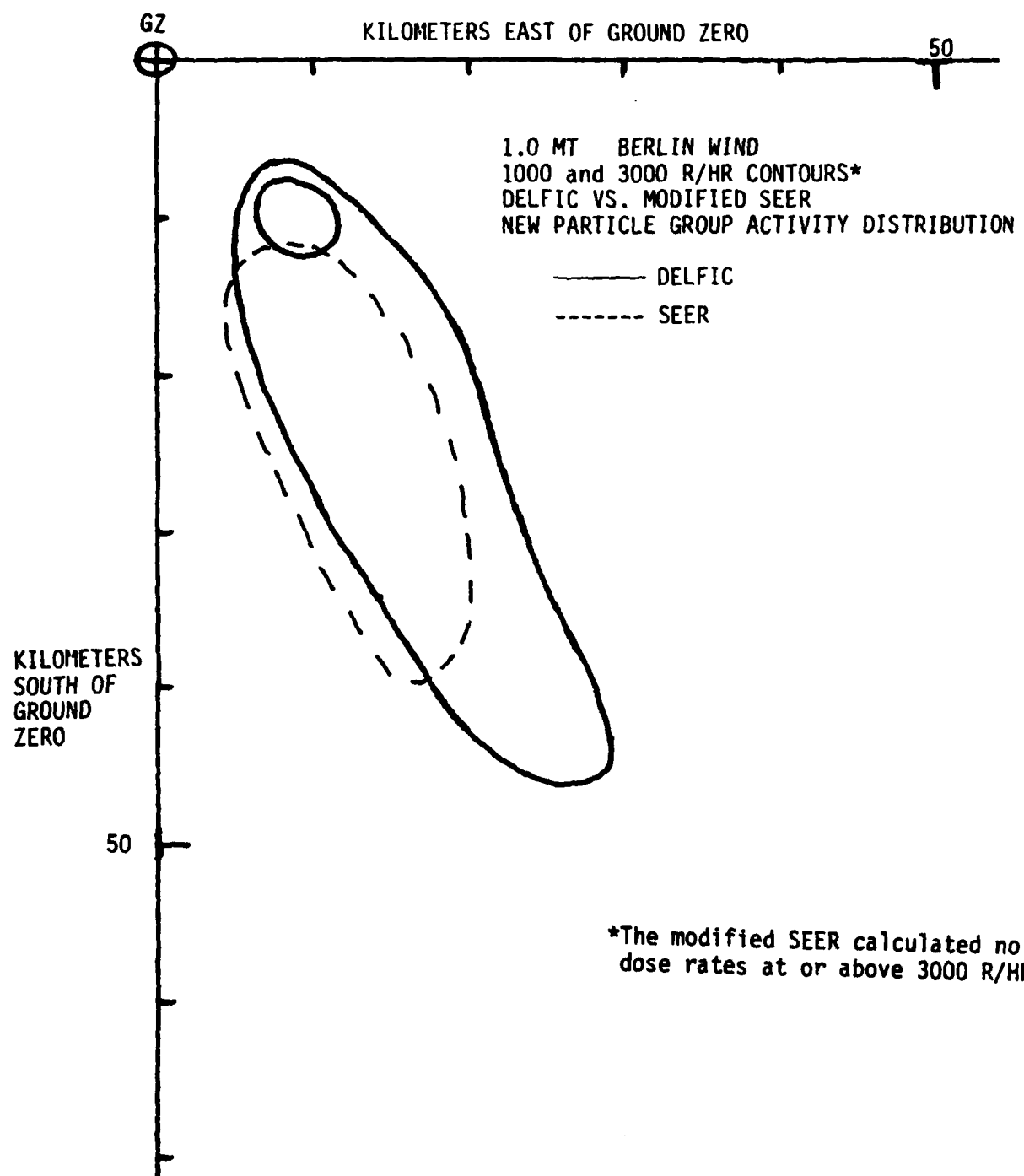


Figure 4-11. 1000 and 3000 r/hr contours, DELFIC vs. modified SEER, new activity distribution.

**Table 4-2. Initial activity values from the literature.**

	<u>Ref. 9</u>	<u>Ref. 7</u>	<u>Ref. 6</u>
Megacuries	450 (p. 5-66)*	530 (p. 453)	----
$(R/HR)/(KT/mi^2)$	--	2900 (p. 390)	3610
$(R/HR)/(KT/m^2)$	---	$7.51 \times 10^9$	$9.35 \times 10^9$
% that is included in "early fallout"	"roughly half" (p. 5-66)	60% (p. 456)	----

All values are normalized to 1 hour after detonation and are for a fission yield of 1 KT. The R/HR values are at a height of 3' above an infinite smooth plane.

\*Reference 9 elaborates on this value with the following footnote:

This value approximates the activity per kiloton in disintegrations per second at one hour. Actual values may range from about 430 to about 460 megacuries, depending on the fissile material and the neutron spectrum that causes the fission. The user may encounter other values in various sources, e.g., 550 gamma-megacuries per kiloton at 1 hour after explosion. This latter is a fictitious, but useful, relationship that relates the fission product gamma source to an equivalent monoenergetic source with an energy equal to the average photon energy of the fission products at 1 hour after the explosion.

represents 65% of the Reference 5 activity value. DELFIC output shows a "fraction down" of 0.568 over a wide range of yields.

For the phase one comparisons, the value of  $6.0775 \times 10^9$  was retained in both versions of SEER. For runs made to obtain the activity in terms of curies/m<sup>2</sup>, a K-factor of 318 megacuries (60% of 530) was used. As discussed previously, the version of SEER now being used with CIVIC has a K factor of only  $3 \times 10^9$  (r/hr)/(KT/m<sup>2</sup>). This low value was introduced in an attempt to produce lower results and offset the tendency of SEER (NEW = 0) to create activity. This overprediction of activity has been discussed above, and can be seen in Figures 4-1, 4-4, 4-5, 4-8, and 4-9.

#### 4-1.4 Discussion of Results

The phase one relative comparison of the two versions of SEER (NEW = 0, 1) is discussed in terms of the 5 criteria: (1) areas enclosed in contours, (2) integrated activity over the map, (3) contour limit distances, (4) appearance of contour plots, (5) run times. The comparisons will be for the SEER runs that used the new (DELFIC) particle group activity assignments (KPGS = 3). For simplicity, the old SEER will be called SEER0, while the modified SEER will be called SEER1. (See Table 4-1 for the values referred to in this section.)

Areas Enclosed in Contours. SEER1 was much closer to the DELFIC values for the 4 contours than was SEER0. The differences (compared to the DELFIC areas) for SEER1 were +14%, +2%, -20%, -100% (respectively for the 10, 100, 1000, and 3000 r/hr contours), while for SEER0 the errors were +72%, +36%, +72%, +94%.

Integrated Activity Over the Map. The maps used to plot the fallout patterns did not cover the entire fallout in any of the 3 cases. The extents of the two SEER maps were the same, while the DELFIC map covered a larger area. However, from the data obtained it is clear that the SEER1 integrated activity is closer to that of DELFIC than is that of SEER0. The differences are -8% for SEER1 and +45% for SEER0. Thus, it can be stated that, within reasonable limits of accuracy, SEER 1 appears to conserve activity.

Contour Limit Distances. SEER1 is somewhat better here, the differences being +2%, +4%, -9%, -100%; while the differences for SEERØ are +1/2%, +37%, +35%, +127%, for the 10, 100, 1000, and 3000 r/hr contours respectively.

Appearances of the Contour Plots. 10 r/hr: Figure 4-1 clearly shows the prime weakness of SEERØ in its method of interpolating, and thus "filling-in" activity where none (or a lesser amount) exists. SEER1 (Figures 4-2 and 4-3) does a better job of showing the variable nature of the fallout field at the outlying regions, although the 10 r/hr contour is by no means identical to that of DELFIC. The "inner" SEER1 contours shown in Figures 4-2 and 4-3 are actually "holes" where the dose rate is slightly less than 10 r/hr.

100 r/hr: Again we see in Figures 4-4 and 4-5 the tendency of SEERØ to overpredict activity. Figures 4-6 and 4-7 show SEER1 to resemble DELFIC more closely.

1000 r/hr: The SEERØ overprediction is again evident in Figures 4-8 and 4-9. In Figures 4-10 and 4-11 we see that changing to the DELFIC particle size class activity assignments dramatically reduced the SEER1 area coverage for the 1000 r hr level from a difference in area from DELFIC of +47% to -20%. The latter is still closer to DELFIC than the +72% of SEERØ.

3000 r hr: SEER1 did not produce a map point at this level of dose rate. While SEERØ did produce 1 map point at 3000 r hr and 2 others above 2500, the location does not coincide with that of DELFIC.

Run Times. The run times for SEERØ and SEER1 are comparable, with the latter being 19% longer for KPGS = 3. However, run times were seen to vary from one run to another, and no attempt was made to streamline the final version of SEER1 or make a methodical comparison over several runs of the "final" version of each (SEERØ and SEER1). Most of the unnecessary diagnostic write statements were removed, however, and the results shown in Table 4-1 are sufficiently representative to state that SEER1 increases the run time over SEERØ by no more than 20% or 25% on the average.

## 4-2 PHASE TWO RESULTS - COMPARISONS WITH CIVIC VERSION OF SEER

Following the initial comparisons of Phase 1, a more comprehensive set of comparisons was made which included the current CIVIC version of SEER (with the adjusted K-factor). A set of previously run, hypothetical shot, cases was available for use in these comparisons (References 1 and 5). These cases covered 11 different winds and 2 yields (50 KT and 1.0 MT). The results that will be discussed here are for the 1.0 MT hypothetical shot yield only, because the 50 KT results were essentially the same and lead to the same conclusions. Because of the data available from References 1 and 5, the results were compared with regard to areas enclosed in the contours (100, 300, 1000, and 3000 r/hr) and contour limit distances only. Contour areas only are shown here because the results and conclusions are the same for contour limit distances.

The plots that are shown in Figures 4-12 through 4-16 show the contour area results in square kilometers for all eleven winds and for the four dose rate contours. SEER contour areas are plotted vs. those of DELFIC (SEER along the ordinate and DELFIC along the abscissa). Areas that are equal (if any) would be plotted along the 45° line shown. All plots shown are for 1.0 MT yield.

From comparison of Figures 4-12 and 4-13 it can be seen that the existing version of SEER comes into much better agreement with DELFIC when the adjusted K-factor is applied. When the particle size group activity distribution is changed to approximate that of DELFIC (Figure 4-14), the results depend upon the dose-rate contour. The SEER-DELFIC correlation is slightly worse at the 100 and 300 r/hr contours, about the same for 1000 r/hr, and somewhat better for the 3000 r hr contour.

The modified SEER (Figure 4-15) provides a dramatic improvement over the old (pre-CIVIC, no adjustment to K-factor) SEER, but is superior to SEER/CIVIC (adjusted K-factor) only for the 100 and 3000 r/hr contours (this superiority is eliminated at 3000 r/hr by use of the DELFIC particle size group activity distribution for SEER/CIVIC). Application of the DELFIC particle size group activity distribution

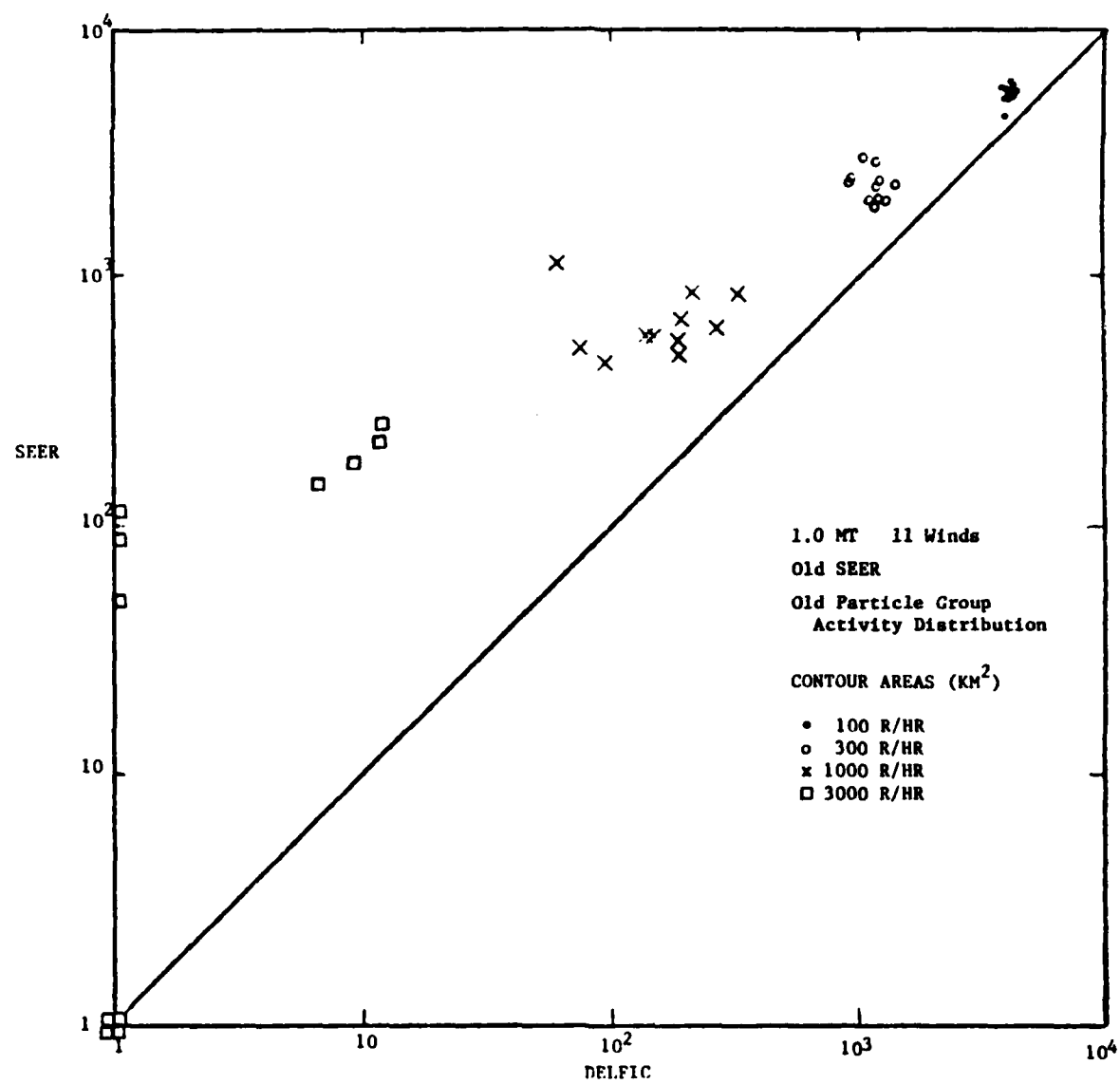


Figure 4-12. Contour areas, DELFIC vs. old SEER.

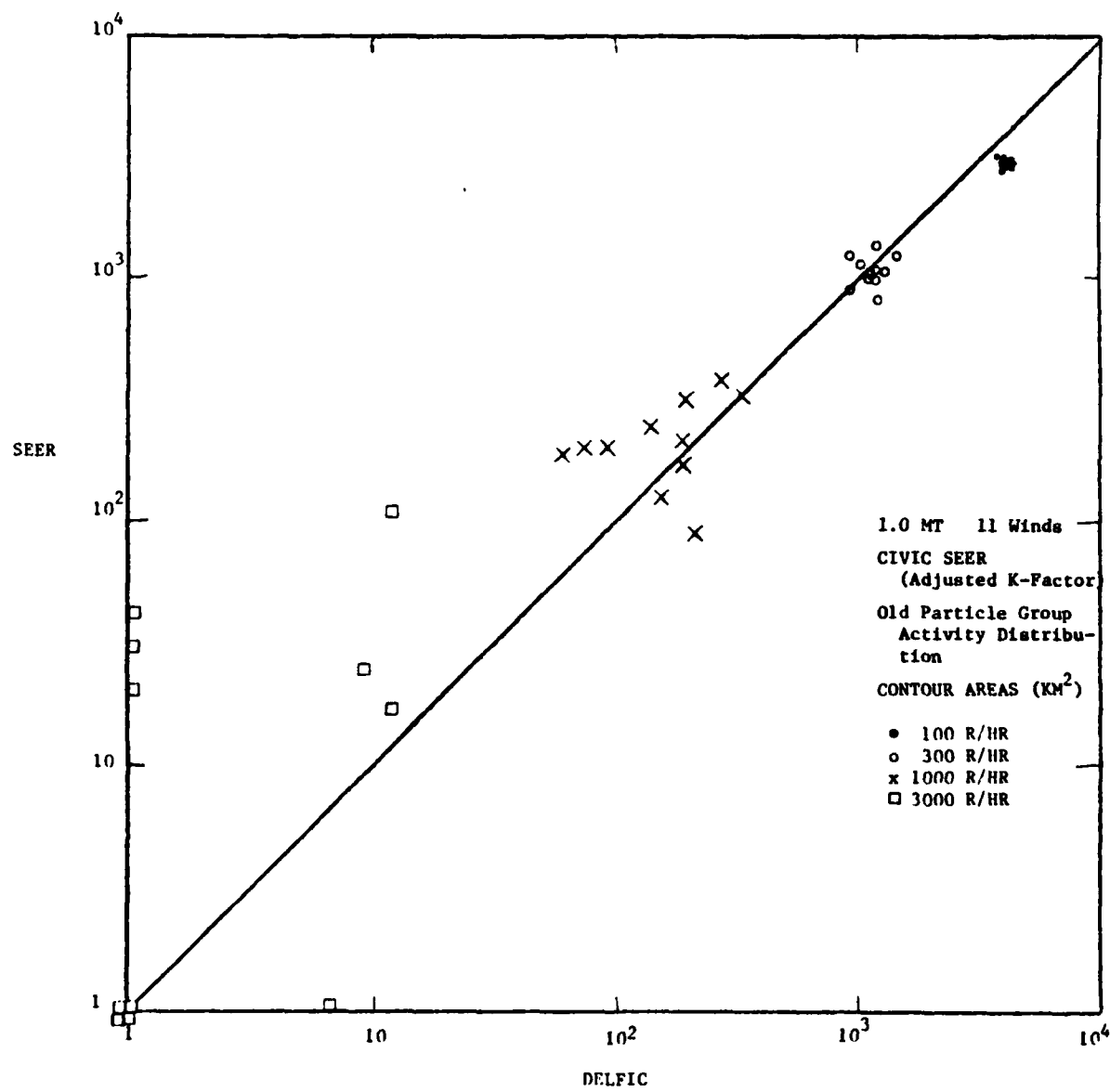


Figure 4-13. Contour areas, DELFIC vs. CIVIC SEER.

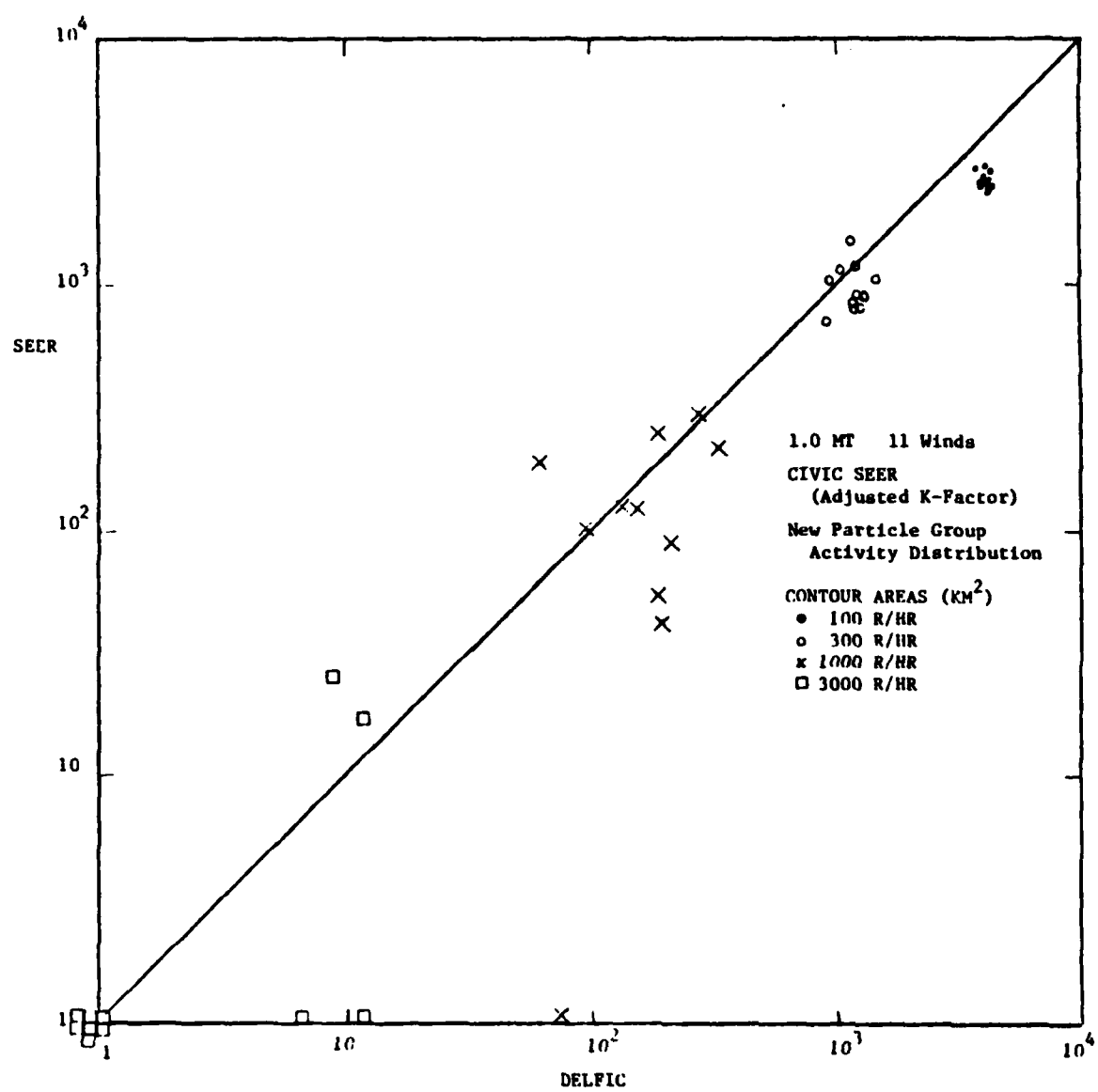


Figure 4-14. Contour areas, DELFIC vs. CIVIC SEER, new activity distribution.

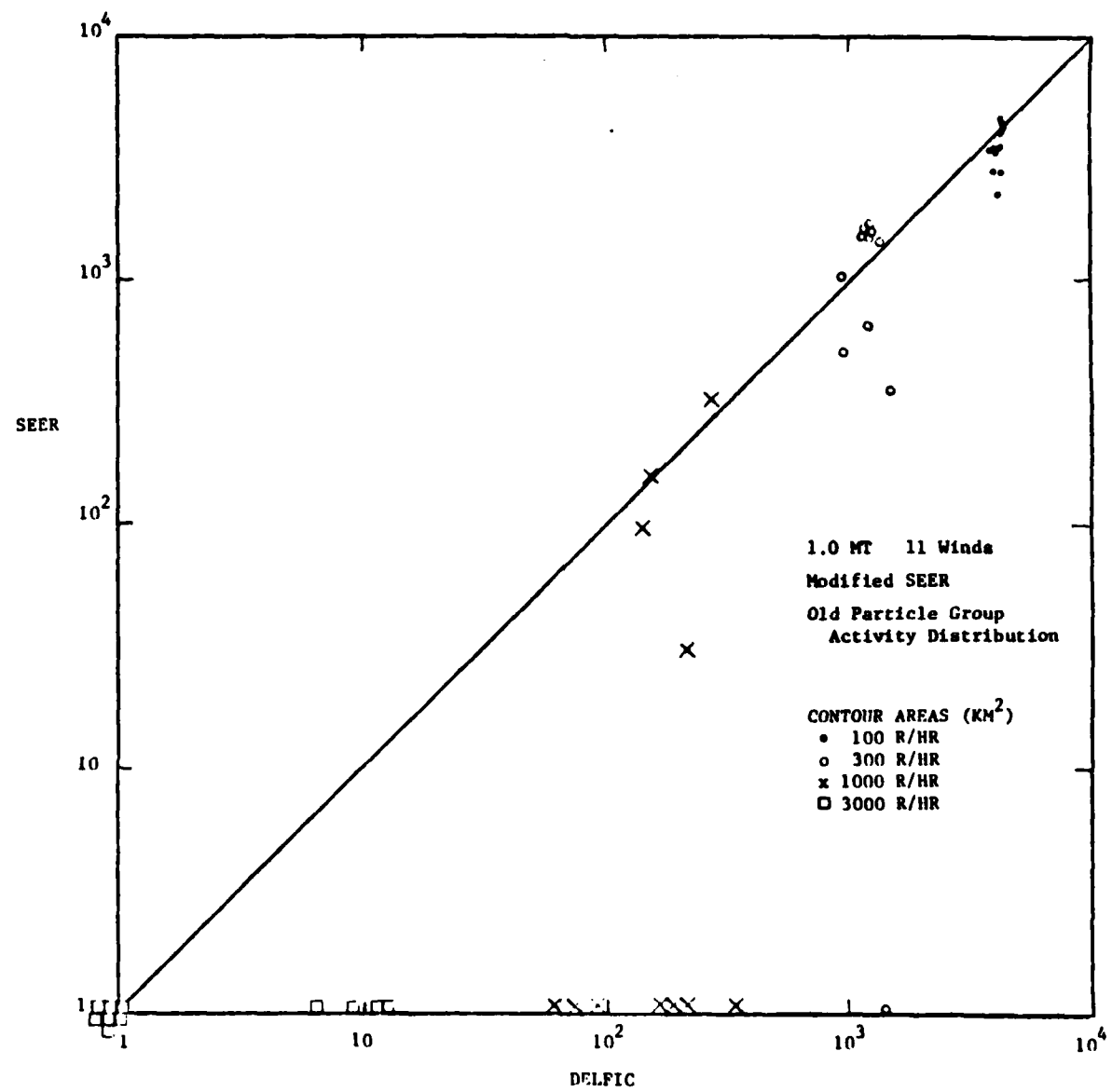


Figure 4-15. Contour areas, DELFIC vs. modified SEER.

to the modified SEER (Figure 4-16) worsens the approximation to DELFIC at the 1000 and 3000 r/hr contours, and therefore accentuates the fact that SEER lacks a model for the cloud stem.

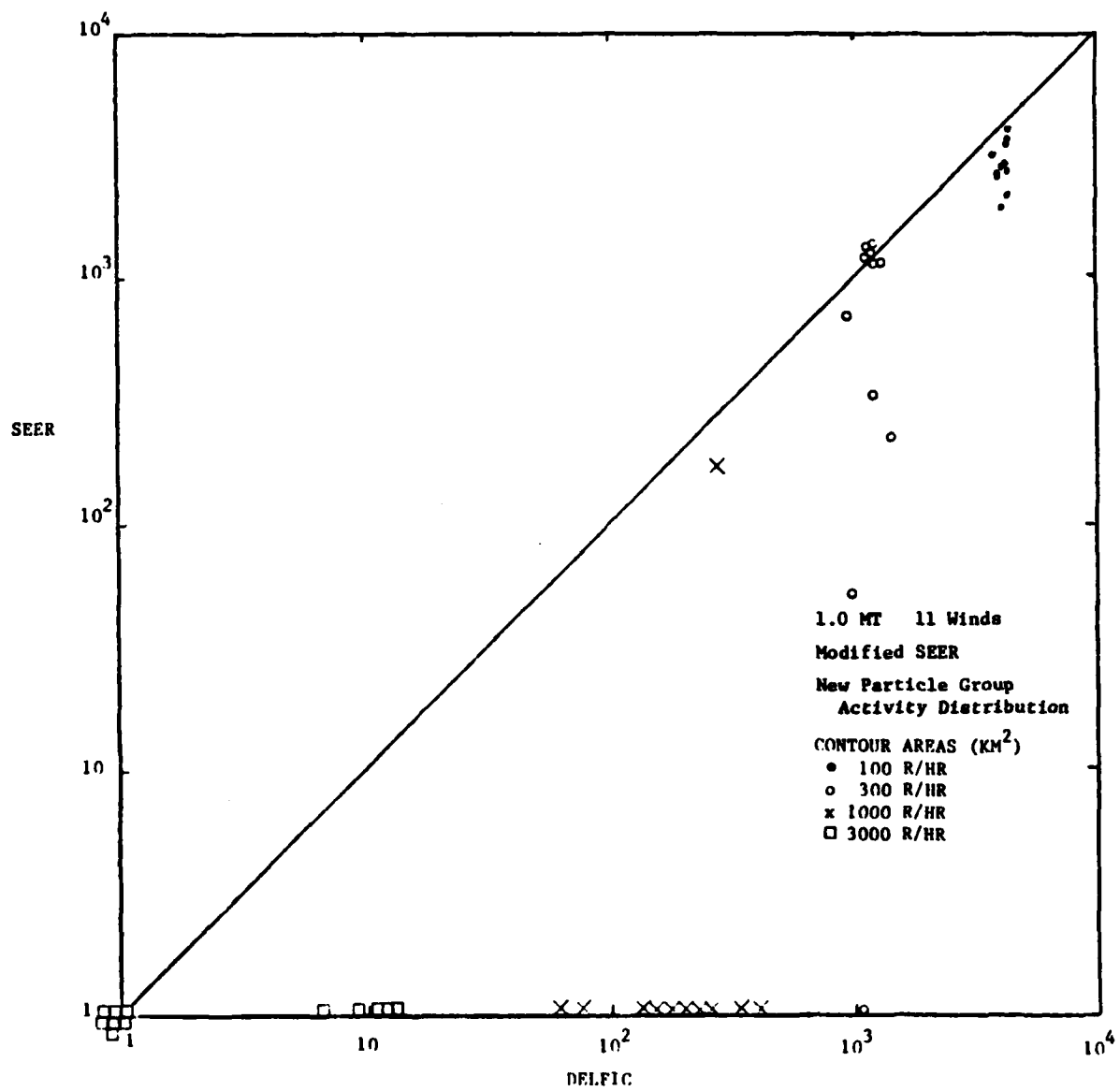


Figure 4-16. Contour areas, DELFIC vs. modified SEER, new activity distribution.

## SECTION 5

### CONCLUSIONS

It is apparent that the modification to SEER reported here has corrected one deficiency of SEER (non-conservation of activity), but has served also to accentuate the other (lack of a cloud stem). The modified SEER has a more accurate physical basis than the current SEER, and therefore is a more faithful representation of activity deposition, given the debris cloud modeled by the code. Additional work would have to be done to overcome the no-stem deficiency. The additional run time of the modified SEER is not considered critical, but great care would have to be exercised in addressing the stem deficiency to avoid significant increases to run time. The overall conclusion of this effort (and considering the results reported in Reference 1) is that, until further work can be done on the modification, the current CIVIC version of SEER with adjusted K-factor is the best available fast-running approximation to DELFIC.

## SECTION 6 REFERENCES

1. Eugene J. Swick, "Fallout Contour Comparison, CIVIC and DELFIC," DNA 5306F, Science Applications, Inc., 8 Feb., 1980.
2. Hong Lee, Paul W. Wong, Stephen L. Brown, "Simplified Fallout Computational Systems for Damage Assessment," DASA-2690, Stanford Research Institute, July 1971
3. Hong Lee, Paul W. Wong, Stephen L. Brown, "SEER II: A New Damage Assessment Fallout Model," DNA 3008F, Stanford Research Institute, May 1972.
4. Hillyer G. Norment, "Analysis and Comparison of Fallout Prediction Models," DNA 4569F, Atmospheric Science Associates, 11 March 1977.
5. Hillyer G. Norment, "Evaluation of Three Fallout Prediction Models: DELFIC, SEER, and WSEG-10," Atmospheric Science Associates, 16 June 1978.
6. C.F. Miller, "Fallout and Radiological Countermeasures," Vol. I, Stanford Research Institute, Jan. 1963.
7. Samuel Glasstone, Philip J. Dolan, "The Effects of Nuclear Weapons," 1977.
8. R.C. Tompkins, "Department of Defense Land Fallout Prediction System, Volume V - Particle Activity," DASA 1800-V, NDL-TR-102, Feb. 1968.
9. "Capabilities of Nuclear Weapons," DNA EM-1, July 1972.
10. Hillyer G. Norment, "DELFIC: Department of Defense Fallout Prediction System, Volume I-Fundamentals," DNA 5159F-1, Atmospheric Science Associates, 31 Dec 1979.

## DISTRIBUTION LIST

### DEPARTMENT OF DEFENSE

Assist to the Sec of Def, Atomic Energy  
ATTN: Exec Assist

Commander in Chief, Atlantic  
ATTN: J22

Defense Intell Agency  
ATTN: DB-4C, Rsch, Phys Vuln Br  
ATTN: RTS-2B

Defense Nuclear Agency  
ATTN: NASF  
ATTN: NAME  
ATTN: RAAE  
ATTN: SPAS  
ATTN: STNA

4 cys ATTN: STTI-CA

Defense Tech Info Ctr  
12 cys ATTN: DD

Field Command, DNA, Det 2  
Lawrence Livermore National Lab  
ATTN: FC-1

DNA PACOM Liaison Office  
ATTN: J. Bartlett

Field Command, Defense Nuclear Agency  
ATTN: FCPR  
ATTN: FCTT, W. Summa  
ATTN: FCTKE

Joint Data System Support Ctr  
ATTN: C-312, R. Mason

Joint Strat Tgt Planning Staff  
ATTN: JLAC  
ATTN: JLK, DNA Rep  
ATTN: JLKS  
ATTN: JP  
ATTN: JPST

Under Sec of Def for Rsch & Engrg  
ATTN: Strat & Space Sys (OS)

### DEPARTMENT OF THE ARMY

Dep Ch of Staff for Rsch, Dev & Acq  
ATTN: DAMA-LSS-N

Harry Diamond Laboratories  
ATTN: SLCHD-NW-P

US Army Ballistic Research Lab  
ATTN: DRDAR-BLA-S, Tech Lib  
2 cys ATTN: DRDAR-BLV-R, J. Maloney

US Army Chemical School  
ATTN: ATZN-CM-AS  
ATTN: ATZN-CM-CS

US Army Nuc. & Chem Agency  
ATTN: Library

### DEPARTMENT OF THE NAVY

Naval Surface Weapons Center  
ATTN: Code F31

### DEPARTMENT OF THE AIR FORCE

Air Force Weapons Laboratory  
ATTN: SUL

Air University Library  
ATTN: AUL-LSE

Air Weather Service, MAC  
ATTN: AWSAE

Strategic Air Command  
ATTN: DEPR  
ATTN: DOCSD  
ATTN: DOTU  
ATTN: DOWE  
ATTN: INAO  
ATTN: NRI/STINFO  
ATTN: XPFS

### DEPARTMENT OF ENERGY

Dept of Energy, Ofc of Mil Appl, GTN  
ATTN: EV, H. Hollister

University of California  
Lawrence Livermore National Lab  
ATTN: L-125, T. Gibson  
ATTN: L-262, J. Knox  
ATTN: Tech Info Dept Library

Los Alamos National Laboratory  
ATTN: M/S634, T. Dowler

Sandia National Laboratories  
ATTN: Tech Lib, 3141  
ATTN: 0332, J. Keizur

### OTHER GOVERNMENT AGENCIES

Central Intell Agency  
ATTN: OSWR/NED

Federal Emergency Management Agency  
ATTN: Asst Assoc Dir for Rsch, J. Kerr

US Army Control & Disarmament Agcy  
ATTN: Ops & Analysis Div, W. Deemer

### DEPARTMENT OF DEFENSE CONTRACTORS

Atmospheric Science Associates  
ATTN: H. Norment

Decision-Science Applications, Inc  
ATTN: Dr. Pugh

Horizons Technology, Inc  
ATTN: R. Kruger

Kaman Sciences Corp  
ATTN: E. Conrad

DEPARTMENT OF DEFENSE CONTRACTORS (Continued)

Kaman Tempo  
ATTN: DASIAC

Kaman Tempo  
ATTN: DASIAC

Pacific-Sierra Research Corp  
ATTN: H. Brode, Chairman SAGE

R & D Associates  
ATTN: C. Knowles

R & D Associates  
ATTN: A. Deverill

Rand Corp  
ATTN: B. Bennett

DEPARTMENT OF DEFENSE CONTRACTORS (Continued)

Rand Corp  
ATTN: P. Davis  
ATTN: R. Rapp

Science Applications Intl Corp  
ATTN: D. Hamlin

Science Applications Intl Corp  
ATTN: J. McGahan  
2 cys ATTN: R. Edwards

SRI International  
ATTN: S. Brown

EAD

DTIC

5- 86